This project has received funding from the European Union's Horizon 2020 research and innovation programme under grant agreement No 773715

Grant Agreement No.: 773715

Project acronym: RESOLVD

Project title: Renewable penetration levered by Efficient Low Voltage Distribution grids

Research and Innovation Action

Topic: LCE-01-2016-2017

Next generation innovative technologies enabling smart grids, storage and energy system integration with increasing share of renewables: distribution network

Starting date of project: 1st of October 2017

Duration: 36+6 months

D5.4 –Validation in relevant environment and results

Organization name of lead contractor for this deliverable: EyPESA	
Due date:	M42 – March 2021
Submission Date:	30 of March 2021
Primary Authors	EyPESA – Joana Alsina, Roberto Fauda, Ramon Gallart UPC – Marc Llonch UdG – Joaquim Melendez
Contributors	EyPESA, UdG, UPC, CS, ICOM, JR
Version	Version 0.3

Dissemination Level		
PU	Public	X
CO	Confidential, only for members of the consortium (including the Commission Services)	

This project has received funding from the European Union's Horizon 2020 research and innovation programme under grant agreement No 773715

Deliverable reviews

Revision table for this deliverable:		
Version 0.1	Reception Date	12th of March 2021
	Revision Date	15th of March 2021
	Reviewers	CS, SIN, UdG
Version 0.2	Reception Date	19th of March 2021
	Revision Date	24th of March 2021
	Reviewers	CS, SIN, UdG
Version 1.0	Reception Date	27th of March 2021
	Revision Date	30th of March 2021
	Reviewers	EST, JR, UdG

This project has received funding from the European Union's Horizon 2020 research and innovation programme under grant agreement No 773715

Table of content

This project has received funding from the European Union's Horizon 2020 research and innovation programme under grant agreement No 773715

Acronyms and abbreviations

BAU	Business As Usual
CEF	Critical Event Forecaster
CEPA	Critical Event Prevention Application
CI	Control Indicator
DAB	Dual Active Bridge
DMS	Distribution Management System
DSO	Distribution System Operator
ESB	Enterprise Service Bus
FN	False Negative
FP	False Positive
FDA	Fault Detection Application
FLA	Fault Localization Algorithm
GOS	Grid Operation Schedule
GW	Gateway
ILEM	Intelligent Local Energy Manager
KET	Key Enabling Technologies
KPI	Key Performance Indicator
LV	Low Voltage
MV	Medium Voltage
MDMS	Meter Data Management Unit
PMU	Phasor Measurement Unit
PV	Photo-Voltaic
PCC	Point of Common Coupling
PED	Power Electronics Device
PQM	Power Quality Monitor
RTU	Remote Terminal Unit
RMS	Root Mean Square
SAIDI	System Average Interruption Duration Index
SS	Secondary Substation
SM	Smart Meter
SCADA	Supervisory Control and Data Acquisition
SG	Switchgear
TN	True Negative
TP	True Positive
TPR	True Positive Rate
TRL	Technology Readiness Level

This project has received funding from the European Union's Horizon 2020 research and innovation programme under grant agreement No 773715

Executive Summary

This report is the last document redacted within the work package dedicated to the validation of RESOLVD and the associated key enabling technologies (KERs) in a relevant environment as fulfillment criteria of achievement of TRL5. It was prepared in collaboration with the different partners involved in the piloting phase.

The selected relevant environment is the already described pilot area (see D1.1 and D5.1) sited in L'Esquirol (Catalunya) and is part of the distribution grid of Estabanell Distribució. Two secondary substations have been conditioned and adapted to deploy RESOLVD hardware that includes a cabinet with power electronic devices, two battery packs and several Phasor Measurement Units (PMU) and Power Quality Monitor (PQM) units. These electronic devices have been integrated with legacy systems through specific communication links. The setup of the pilot has been completed with the integration of the grid operation software infrastructure, i.e. SCADA and advanced metering infrastructure (ie. AMI and MDMS). These, together with the new software components developed in RESOLVD, provide the enhanced observability and management capabilities to the pilot area. The overall integration has been done with an Enterprise Service bus (ESB) and under strict cybersecurity criteria.

This document provides summary of the final results obtained from the tests carried out in real scenarios in order to evaluate the performance of the developed technology. The completed tests were intended to study the impact of the RESOLVD technologies regarding efficiency, operation/planning, and quality of service in a low voltage (LV) grid.

Thus, regarding the effect of the technology in the grid efficiency, the waveform quality has been proved to improve, by compensating reactive currents and harmonics, and the power losses have been reduced by peak shifting and maximizing local consumption of RES locally generated by PV panels. The tests related to grid operation, proved that critical events as well as faults in the grid were accurately detected, in specifically generated scenarios. After successfully detecting these events, the grid operation schedule (GOS), provided planning solutions always with the minimum switching operations in the grid. When it comes to quality services, tests were performed to improve voltage levels, by injecting or consuming active and reactive power, as well as to control voltage variations and reverse the power flow during periods of time when large differences between demand and production occur.

The last operational test performed, confirmed the possibility of exploiting RESOLVD technology to operate part of the LV grid in island mode. For that purpose, the power electronic device (PED) is operated as voltage source capable of maintaining frequency and feeding consumers directly from the storage system.

Finally, regarding the cybersecurity evaluation, security checks were performed for each component of RESOLVD when ready for the integration and recommendations to eliminate security issues as well as individual advices were communicated to the responsible partners. All the components were integrated following those considerations and tests reported in this deliverable were obtained with all the components fully integrated.

This project has received funding from the European Union's Horizon 2020 research and innovation programme under grant agreement No 773715

1. Introduction

1.1. Objectives

The purpose of this document is to provide a description of the pilot and involved elements, the different test configurations that have been used, and to present the main calculations and results of these tests. This will be done through the previously identified KPIs, following the suggested methodology and formulas described previously in D5.1.

Moreover, it will be used to identify and analyze the main challenges faced during the testing period and to describe the exploitation opportunities and potential of the developed technologies.

1.2. Partner contributions

This document presents a holistic analysis of the project results, gathering both the methodology and numerical results. The collaboration of all consortium partners was therefore imperative. Each consortium partner has contributed to the deliverable, as shown in Table 1:

Table 1 Contribution of partners to Deliverable D5.4

Partner	Contribution
EyPESA	Leading contributor. Author of sections 1, 2, 3, 4.4, 4.5, 4.6, 4.9, 6 and 7
UPC	Description of methodology and results calculations of sections 4.1, 4.3 and 4.11
UdG	Description of methodology and results calculations of sections 4.2, 4.7 and 4.8
JR	Description of methodology and results calculations of section 5
CS	Description of methodology and results calculations of section 4.9

1.3. Report structure

The document is organized according to the following structure. First, a brief presentation of the pilot site, adaptation and operation configurations. It follows a general overview of the schedule followed during the testing period. After that, Chapter 4 presents the main section of the report, deepening on the calculations and the results obtained from the data collected during the last months. For that, a specific subsection has been dedicated to each one of the previously agreed indicators which are documented in D5.1, presenting the followed methodology, calculations, and major outcomes. Before the last section with the main conclusions, the potential future opportunities of the project outcomes will be introduced for further development.

2. Pilot elements and configuration

RESOLVD project's Key Enabling Technololgies (KETs) are being tested in the low voltage grid of a village called L'Esquirol, in the north of Catalunya. As seen in Figure 1, this grid is composed of two three-phased lines, deriving from two different secondary substations, (SS) SS-A and SS-B. In both there are consumers and generation points (PV installations). Table 2 shows the technical parameters of the two substations feeding the pilot. Initially, the two three-phase transformers of the secondary substations had different neutral connection: one was delta type whether the other presented as a star connection. In order to allow a more flexible operation, including a ring configuration, one of these transformers was substituted. Thus, finally the pilot has been equipped with two transformers, with Dyn11 connection, with star connection at LV level. It should be noted that the MV/LV transformers are oversized with respect to the load of the area. This is because some years ago (at the proposal stage), the two substations had to supply two high-load factories that now are closed.

Table 2 Specifications of the secondary substations

Secondary substation	SS A	SS B
Transformer rated power	250 kVA	630 kVA
Total contracted power	138,6 kW	127,8 kW
Contracted power of line in the pilot	58,3 kW	56,9 kW
PV power installed in the pilot	12,5 kW	9,9 kW

This pilot area has undergone additional changes in order to allow testing specific scenarios and use cases.

- First, the two radial lines were connected through a link cable that allows to create a ring shape, as it can be seen in Figure 1. In order to remotely control and reconfigure the grid moving borders, three fuses were substituted by motorized 3VA Siemens switchgears, with a performance range from 16 A to 1000 A.

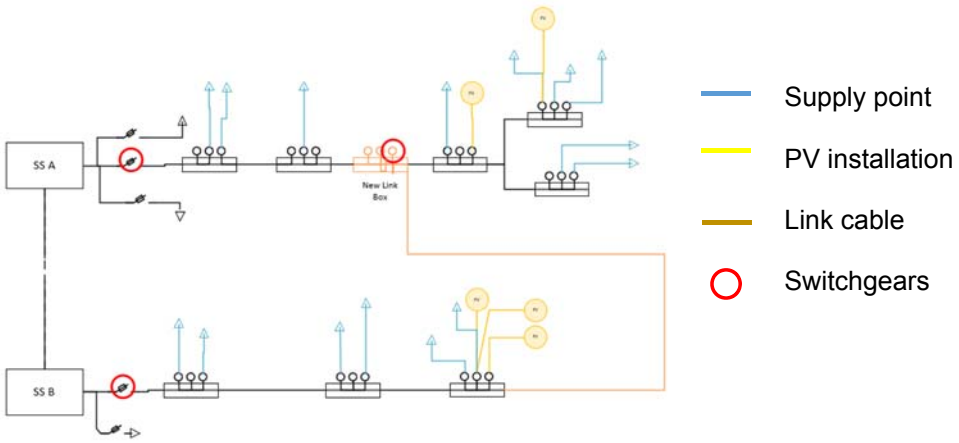

Figure 1 Single line diagram of the pilot area

- In order to analyse the energy exchanged between the batteries and the grid, and to evaluate the performance and efficiency of the technology, smart meters were installed at the beginning of the two feeders and in the point of common coupling the power electronic device (PED).

The PED together with two battery packs and corresponding instrumentation equipment are the main hardware technologies developed in the project. It has been developed and provided by UPC and installed in the SS-B. This location has been selected for space reasons, as it consists of a two floor-building, with an empty second floor.

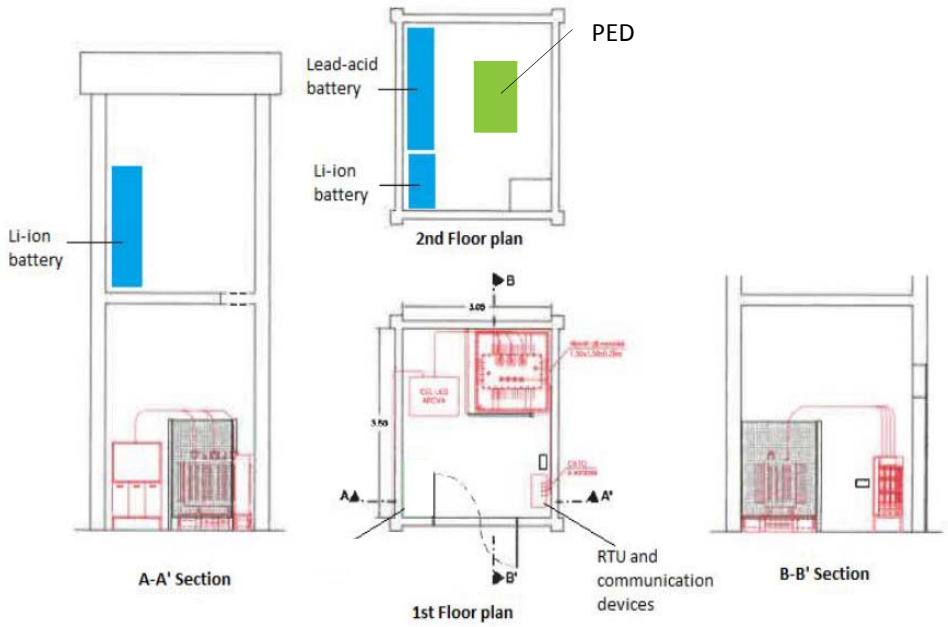

Figure 2 Situation of the hardware inside the substation

The PED, the Lithium-ion and the Lead-acid batteries are installed on the second floor as sketched in Figure 2. The inclusion of different types of batteries, permits to take advantage of the main performances of each one depending on the service to provide As described previously in D2.3, the lithium-ion pack provides 30 kWh and the lead-acid one 18 kWh, and the technical specifications of both types are summarized in Table 3 and Table 4.

Table 3 Characteristics for the lithium-ion mattery pack based on the information provided by manufacturer and laboratory test

Item	Description
Manufacturer	FENECON
Model	C PLUS 25
Nominal capacity and voltage	87 Ah (C/3); 348 V nominal voltage for the whole pack, 3.2 V per cell.
Maximum discharge current	90 A (1C)
Charge resistance, R_c (simple model)	0.2121 Ohm
Discharge resistance, R_d (simple model)	0.2012 Ohm
Discharge temperature	-15 ºC to 50 ºC (25 ºC recommended)
Charge temperature	0 ºC to 40 ºC (25 ºC recommended)
Charging current for cycle use	Voltage limits for the whole pack are set between 302 V and 387 V (corresponding to 2.8 V and 3.65 V per cell)
Efficiency (round trip)	94.7%

Table 4 Characteristics for the lithium-ion mattery pack based on the information provided by manufacturer

Item	Description
Manufacturer	Ultracell
Model	UCG75-12
Nominal capacity and voltage	75 Ah (C/10) @ 12 V per battery; 240 V for the whole pack.
Maximum discharge current	900 A
Internal resistance	6.6 mOhm per battery; 0.1320 Ohm for the whole pack (and the resistance of the connectors and wires should be also added).
Discharge temperature	-15 ºC to 50 ºC (25 ºC recommended)
Charge temperature	0 ºC to 40 ºC (25 ºC recommended)
Charging current for cycle use	Initial charging current less than 22.5 A. Per battery, final voltage between 14.4 V and 15.0 V at 25 ºC (between 288 V and 300 V for the whole pack). This value is corrected with temperature coefficient -30 mV/ºC
Efficiency (round trip)	91.6%

The remote terminal units (RTU) and the gateway (GW) devices required for the integration of PED and batteries with the SCADA are located on the ground floor. This distribution allows establishing a specific floor for the DSO specific assets and it is also easier for the user to control the whole system. To sustain and distribute their weight over the floor, a metallic support was constructed and located under the energy storage system. The batteries and the battery management system (BMS) are electrically connected to the PED by a cable and the link from LV switch gear and the feeder-2 goes through the floor.

The new instrumentation technologies, include Phase Measurement Units (PMU) and the Power Quality Meters (PQM), developed and provided by ComSensus were installed on both the low voltage and the medium voltage level. PQMs serve to analyze the power waveform and thus need connected voltage and current measurements inputs. The voltage and current ranges permitted by these devices required the installation of voltage and current transformers and Rogowsky sensors as well.

With all these technologies, the main goal is to evaluate the impact of the RESOLVD solution in the distribution grid, mainly at LV (400 V) feeder level. Several tests were planned to be performed in the area regarding efficiency, planning and quality service to cover the initially planned scope summarized in Table 5.

Efficiency is mainly measured as an improvement of the energy profile at the SS level without affecting the consumer behavior, whereas the reduction of power losses in the local grid is mainly associated to a better waveform quality since LV lines are very short. Installing the measurement equipment in both, upstream and downstream, of the PED PCC allows quantifying the improvement introduced by the PED.

When it comes to quality service, voltage profiles improvement, critical events prevention and island mode operation is studied in the pilot area. To do so, the PED and batteries installed at the SS will be crucial to smooth the voltage variations by exchanging power with the grid, increasing, or decreasing the voltage to compensate the consumption or generation variation. The measurement equipment will be again used to analyze the impact of these actions.

Table 5 Summary of indicators to be tested

Category	Title	Measurement units
Efficiency	Power loss reduction due to waveform quality improvement	% kWh/year
	Improvement of the energy profile in the secondary substations	- Losses T&D (%) - Locally generated energy use (%) - Maximum peak (%)
Planning	Efficiency rate of the PED and the energy storage system	%
	Increase of DERs hosting capacity in LV network	%kW with respect to the current maximum limit
	Reduction of DSO investment.	% with respect to situation without RESOLVD
	DSO operation expenditures with respect to the BAU solutions	% with respect to situation without RESOLVD
Quality of service	Percentage of improvement in line voltage profiles with power injection and consumption	% C/kW-V/kVA
	Rate of prevented critical events in the LV grid due to forecasting and remote control of grid actuators	- Precision of forecasting (%) - TRR of forecasting (%) - Effectiveness of the mitigation action (%)
	Quality of online event detection in LV grid	- Accuracy(%) - Precision (%) - Miss Detections (%) - False Alarms(%) - Detecting time (s) - Informing delay (s)
	Quality and time needed for awareness and localization of grid fault MV grid	- Efficiency (%) - Localization accuracy (%) - Times (%)
	Quality of LV grid operation in island mode	- Duration [hours] - Reason for island mode interruption (%) - Waveform quality
	Waveform quality in LV grid	Fulfillment/unfulfillment of waveform quality standards

2.1. Grid configuration

The following schema represents a simplified view of the pilot grid. It can be observed the two secondary substations, labeled SS-A and SS-B respectively, the location of PED and batteries at the beginning of a line in the SS-B and the three switchgears that allows operating the grid and changing its configuration.

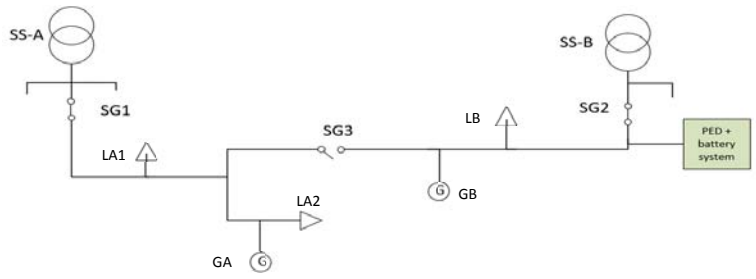

Figure 3 Simplified schema of the pilot grid

The following table summarises the basic characteristics of the different configurations that results of operating the three switchgears and the interest for the calculation of specific KPIs mdescribed in Section 4.

Table 6 Grid configurations according to switchgears with PED connected

SG1	SG3	SG2	Configuration description	Observations	KPIs
0	**0**	**0**	Island mode LB fed by PED + batteries (and GB). LA without service,	Not allowed during the test	-
0	**1**	**0**	Island mode, without loss of customers LA1&2 + LB fed by PED + batteries (and GA+GB)		KPI9
0	**0**	**1**	LB connected to SS-B Loss of LA1&2: disconnected from the main grid.	Not allowed during the test	-
0	**1**	**1**	LA1&2 + LB fed by SS-B.	This state allows feeding LA and LB from SSB and perform peack shaving and battery energy management. Maximum profit of PV generation (GA and GV)	KPI2, KPI6
1	**0**	**0**	LB disconnected from the main grid.	Not allowed during the test	-
1	**1**	**0**	LA1&2 + LB fed by SS-A. PED at the end of the line	This configuration set the PED at the end of the line.	KPI4
1	**0**	**1**	Normal operation mode, PED is connected the begiing of SS-B	This is the traditional model to operate lines radially: each one from its substation (LA – SSA, LB – SSB).	KPI1 CI03
1	**1**	**1**	Ring configuration	Ring operation: all the loads supplied from both sides (SG3 connected). Due to different volatge adjustments at the secondary SS-A and SS-B, this configuration produces high currents. This circumstance is used to 'emulate ' high impedance faults (KPI7: fault detection tests) without tripping protections and affecting supply.	KPI7 (transitions from 101, 110 and 011)

This project has received funding from the European Union's Horizon 2020 research and innovation programme under grant agreement No 773715

3. Timeline and calendar overview

Despite the RESOLVD project was initially planned as 36 months project, ending in Sept 2020, its duration was extended 6 months to end in March 2021. This mean that integration and piloting were performed during the COVID1-19 pandemic situation resulting in severe mobility and pilot access restrictions. This context forced to reconsider the planning of the integration and piloting phases avoiding physical the presence of partners in the pilot due to, on one hand, the traveling restrictions imposed by the lockdown and on the other hand the consideration of electrical grid as critical infrastructure reducing operations to those oriented to assure supply.

This scenario obligated to continuously (week by week) adapt planning of piloting and testing tasks to the lockdown conditions and internal procedures of the DSO.

Thus, due to COVID-19 restrictions and other restrictive issues that will be mentioned later, the on-site tests were performed in the period December 2020 - March 2021, later than initially planned as soon as the conditions were permissive enough to launch tests in the real scenario.

Before December, the tasks focused on installation and setup preparation, combining laboratory and on-site tasks when allowed. Main on site tasks involved the installation of the required equipment such as the new transformer, switchgears (SG), PQMs and PMUs and the corresponding measurement transformers. AS exposed, these required a modification and extension of the first proposed calendar. The PED was already in the site when the lockdown started; however, it was not fully integrated, and this task took more time than expected due to the restrictions to the access.

The first key performance indicator (KPI), regarding power losses reduction due to waveform quality improvement, was carried out the 11th of December, and continued the following week. During the second half of the month, tests were performed regarding KPI2, KPI 5 and KPI6.

After Christmas holidays, the testing phase was resumed on the 12th of January, when KPI 7 and KPI 9, regarding quality of online event detection in LV grid and LV grid operation in island mode, respectively, were tested on site. The last week of January and the first days of February were used to repeat some of the already tested KPIs, this time for a longer period of time.

For all these testing days, both UPC and EyPESA were on field, while UdG, ICOM and CS were providing remote and online support as well as collecting and sharing the generated data.

DECEMBER 2020						
Mon	Tue	Wed	Thu	Fri	Sat	Sun
30	**01**	**02**	**03**	**04**	05	06
					KPI2	KPI2
07	**08**	**09**	**10**	**11**	12	13
KPI2	KPI2	KPI2	KPI2	KPI2 KPI 1	KPI2	
14	**15**	**16**	**17**	**18**	19	20
		KPI 1 KPI 6				
21	**22**	**23**	**24**	**25**	26	27
KPI 5		KPI 2				
28	**29**	**30**	**31**	01	02	03

Figure 4 December overview of performed tests

JANUARY 2021						
Mon	Tue	Wed	Thu	Fri	Sat	Sun
				1	2	3
4	5	6	7	8	9	10
11	12	13	14	15	16	17
	KPI 7 KPI 9					
18	19	20	21	22	23	24
25	26	27	28	29	30	31
	KPI7					

Figure 5 January overview of performed tests

FEBRUARY 2021						
Mon	Tue	Wed	Thu	Fri	Sat	Sun
1	2	3	4	5	6	7
	KPI2					
8	9	10	11	12	13	14
	KPI 2					
15	16	17	18	19	20	21
22	23	24	25	26	27	28
1	2	3	4	5	6	7

Figure 6 February overview of performed tests

4. Test results and Key Performance Indicators

4.1. Test and KPI 1: Power losses reduction due to waveform quality improvement

The objective of this KPI is to evaluate the power transport loss reduction due to the improvement of the waveform quality. The improvement of the waveform quality refers to the compensation of reactive currents, the cancelation of harmonic currents and the balancing of three-phase currents of the power flow upstream via the PED. In this sense, it is expected that the whole current demand at the secondary substation decreases, reducing the losses associated to transmission and distribution. In the pilot area, the point established as the border between primary and secondary distribution system is the point of connection of the LV feeder in SS030, right upstream the PCC of the PED.

4.1.1. Followed methodology

The test is based on the real measurement of the three phases' current reduction in the pilot area of reference. The measurements have been taken with two identical power quality analyzers (two PQMs provided by Comsensus) installed upstream and downstream of the PCC of the PED as pointed in Figure 7. This configuration makes it possible to represent the impact of the PED on the power quality.

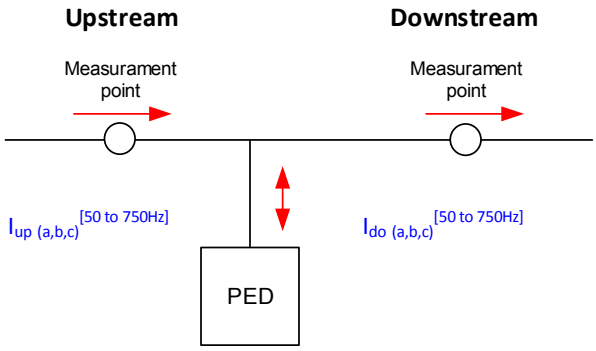

Figure 7 Configuration of analyzers with respect to the PED, to measure the power quality improvement

Therefore, through the two power quality analyzers located upstream and downstream of the PED, it is possible to pick the three phases RMS currents for their subsequent treatment. The expected information for each time value (t) and phase (x) is included in Table 7.

Table 7 Measured currents in KPI-01

Input	Description
$I_{50Hz}(t,x)$	Fundamental three-phase RMS currents (at 50 Hz)
$I_{150Hz}(t,x)$	Third harmonic three-phase RMS currents (at 150 Hz)
$I_{250Hz}(t,x)$	Fifth harmonic three-phase RMS currents (at 250 Hz)
$I_{350Hz}(t,x)$	Seventh harmonic three-phase RMS currents (at 350 Hz)
$I_{450Hz}(t,x)$	Ninth harmonic three-phase RMS currents (at 450 Hz)
$I_{550Hz}(t,x)$	Eleventh harmonic three-phase RMS currents (at 550 Hz)
$I_{650Hz}(t,x)$	Thirteenth harmonic three-phase RMS currents (at 650 Hz)
$I_{750Hz}(t,x)$	Fifteenth harmonic three-phase RMS currents (at 750 Hz)

The KPI_1 is calculated as a percentage of losses reduction. The following equation shows that the electrical losses (P_{losses}) are proportional to the product of conductor resistance or the system equivalent resistance (R_{eq}) and the square of the total current (I_T).

$$P_{losses} = R_{eq} \cdot I_T^2$$

Therefore, it is assumed that the equivalent resistance is the same for both situations, with and without PED contribution.

$$KPI\_01 = \frac{I_{T_{\text{upstream}}}^2}{I_{T_{\text{downstream}}}^2}$$

Where the total current per each side of the PED is:

$$I_T = \sqrt{I_{50Hz}^2 + I_{150Hz}^2 + I_{250Hz}^2 + I_{350Hz}^2 + I_{450Hz}^2 + I_{550Hz}^2 + I_{650Hz}^2 + I_{750Hz}^2}$$

Finally, it is important to note that there are three-phase currents, so it is necessary to add them in a unique term (I_T), and it is necessary to analyze the evolution of KPI along the time.

4.1.2. Calculations and results

The data was collected on the 16th of December. The PED worked in 'Grid mode', balancing currents and reducing the harmonics and reactive power from 11:52 until 15:00. The grid configuration was set to [101], meaning that the PED was only filtering the current of line 2 of SS-B, as can be seen in Figure 8.

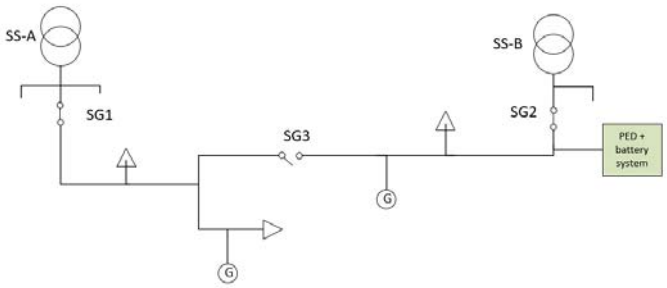

Figure 8 Configuration with SG2 and SG1 closed, SG3 open

The results are depicted in Figure 9, where the three phase currents, upstream (GRID) and downstream (LOAD) of the PED, can be seen on the left. On the right, the squared current difference between upstream and downstream is also depicted in order to integrate it and obtain the energy saved per unit of line resistance.

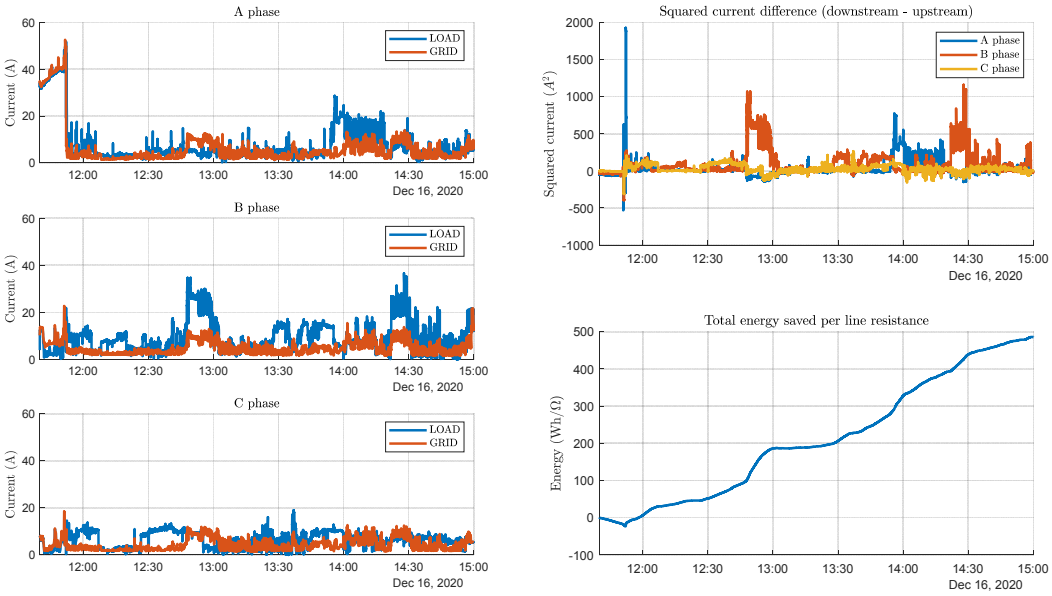

Figure 9 Results of the KPI 1

After compiling data, KPI 1 has been reformulated in order to obtain a more representative value. Considering that the losses are proportional to the square of the current:

$$P_{losses} = R_{eq} \cdot I_T^2$$

The reduction of losses caused by the PED is:

$$\Delta P_{losses} = R_{eq} \cdot \left(I^2_{T_{\text{downstream}}} - I^2_{T_{\text{upstream}}} \right)$$

With this, KPI 1 can be defined as the amount of power saved per unit of resistance, as follows:

$$KPI\ 1 = \frac{\Delta P_{losses}}{R_{eq}} = avg\left(I^2_{T_{\text{downstream}}} - I^2_{T_{\text{upstream}}} \right)$$

Finally, viewing the energy saved during 3 hours of test in Figure 9, the final impact energy saved per unit of resistance is:

$$KPI\ 1 = \frac{500}{3} = 166.7\ \frac{W}{\Omega}$$

4.2. Test and KPI 2: Improvement of the energy profile in the secondary substations

The presence of high peaks on the power profile of the substations has disadvantages such as high-power losses in the transmission lines, an increase in maintenance costs or high emissions of carbon dioxide. The integration of battery storage systems in the grid is on of the most promising strategy to modify the load demand profile of an aggregation of prosumers. Performing peak shaving on the distribution feeders can have several benefits at different levels, reducing the before mentioned disadvantages and even the economic costs, since typically with a high demand of energy the price is higher.

The goal of this KPI is to analyze how energy profiles at the substations can be improved by managing energy locally generated, scheduling the charge and discharge of batteries installed in the pilot.

4.2.1.Followed methodology

Basic guidelines described in D5.1 have been followed. Assuming that the transport losses within the feeder can be neglected, the net energy profile of a feeder is the balance between consumption, generation, and contribution of the PED, that also includes the battery system.

$$\vec{E}_P = \vec{E}_D - \vec{E}_G + \vec{E}_{PED}$$

Where,

$\vec{E}_P$: Energy profile or flux at the substation is the net exchange between the feeder and the substation.

$\vec{E}_D$: Demanded energy for consumption;

$\vec{E}_G$: Energy generated by DERs;

$\vec{E}_P$: Energy exchanged by the PED.

The computation of these energy flows has been done in a daily base, since this is the time frame managed by the Grid Operator Scheduler (GOS). It is important to clarify that imported energy is considered at the substation level, when $\vec{E}_p$>0 and exported energy is considered when $\vec{E}_p < 0$.

Indicators

In a daily profile the following indicators are defined:

- Total (daily) exchanged energy: $E_T = \sum_{i=1}^{24} |E_P(i)|$
- Total (daily) imported energy: $E_I = \sum_{i=1}^{24} E_P(i)$ with $E_p(i) > 0$
- Total (daily) exported energy: $E_E = \sum_{i=1}^{24} E_P(i)$ with $E_p(i) < 0$
- Peak, or maximum daily value: max ($\vec{E}_p$):
- Variability: $V[0,1] = \sum_{i=0}^{24} \frac{\left|\frac{E_T}{24} - E_P(i)\right|}{E_T}$
- Losses in the PED + Battery: $\vec{E}_L = \vec{E}_{LC} + \vec{E}_{LD}$
  That is the consumption of power electronics plus the losses incurred by the battery during charge and discharge operation.

The following model, identified by UPC, has been used in this study to estimate the associated losses at every charging (P_{BC}) / discharging (P_{BD}) 1h step. The constant terms are mainly associated to the operation of the battery and the power electronics, respectively.

$$\vec{E}_{LD} = 0{,}0694 \cdot |P_{BD}| + 0{,}6981$$

$$\vec{E}_{LC} = 0{,}0437 \cdot |P_{BC}| + 0{,}5866$$

Set up

For this test energy demand and generation forecast is required. Therefore, forecasting models for every smart meter (SM) in the pilot have been trained. These models have been used to forecast the generation and demand profiles required by the GOS as inputs. The GOS computes the optimal schedule according to the forecasts and adapts the output according to the losses model of the batteries in order to avoid discharging due to PED and batteries consumption. The schedule provided by the GOS indicates the hourly profile of charge/discharge for the battery and an estimation of the state of charge of the batteries.

Following settings have been used for testing:

- Grid Configuration: [011]
- Schedule options: ESS (Only Batteries), Nu=0.8
- Battery adjustments:
  - Capacity: 25kWh (Only Ion-LI is operative)
  - Default SoC: 0.55 (update is sent by SCADA)
  - Max charge/discharge rate: 0.5 Capacity

Execution

As presented before in the calendar overview, one-week test was performed (05/02/2021-12/02/2021). Table 8 summarises the main energy indicators, used as baseline, obtained from the forecasted consumptions and generation for the whole week.

Table 8 Baseline: energy balance and indicators without applying battery schedule

No BAT	05/02/2021	_2021-02-06	07/02/2021	08/02/2021	09/02/2021	10/02/2021	11/02/2021	12/02/2021
Total imported (Wh)	172404	201896	241030	197477	222407	179200	195473	217075
Total exported (Wh)	-9585	0	0	-5867	0	-8749	-9667	0
Total exchanged (Wh)	181988	201896	241030	203344	222407	187949	205139	217075
Max Peak	15598	15974	16389	16927	15694	14254	16100	14076
Peak reduction (%)								
Total variability	0.61	0.38	0.20	0.50	0.28	0.52	0.52	0.25
Total Generation	82460	60620	35280	75940	48670	85510	94560	36720
Total Energy (imported+ generation)	254864	262516	276310	273417	271077	264710	290033	253795
Local Consumption (Total-Exported)	**245279**	**262516**	**276310**	**267550**	**271077**	**255961**	**280366**	**253795**

Negative values of energy refer to exported energy. Thus, the total exchange corresponds to the addition of total imported and exported, without sign. Variability and peak have been computed as described in the previous subsection.

4.2.2. Calculations and results

A typical execution of the GOS results in a sequence of set points as depicted in Figure 10 (right), resulting in a flatten energy profile (left). Evolution of battery state of charge and associated losses can be observed in Figure 11.

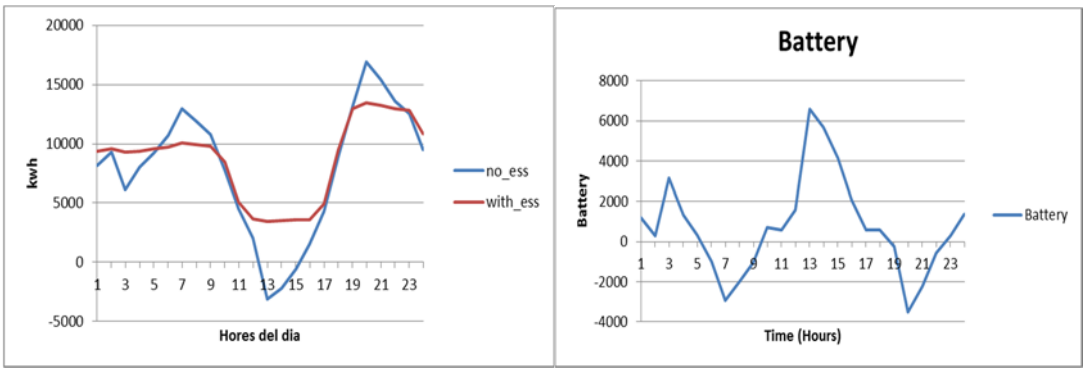

Figure 10 Energy profile (blue without GOS / red with GOS) and battery charge/discharge set points

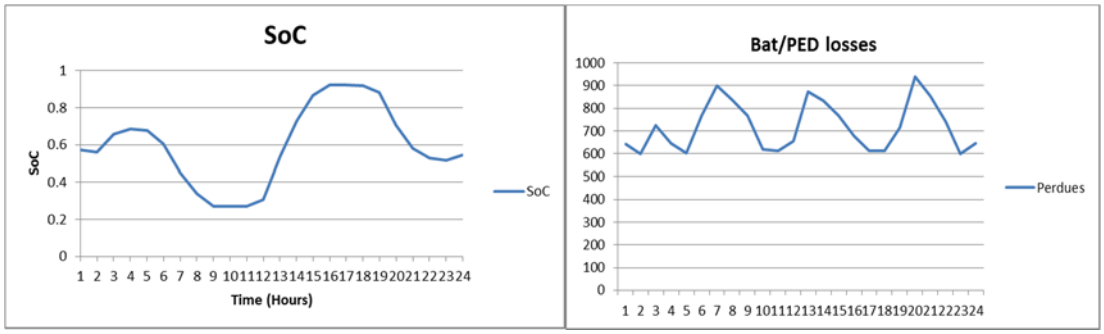

Figure 11 Evolution of State of Charge (left) of the battery and losses (in kW)

Table 9 shows the aggregated daily values of energy and indicators and Table 10 summarises these results in weekly time base as aggregated and average values.

Table 9 Results applying battery schedule: daily energy balance and indicators

GOS (Nu=0.8)	05/02/2021	_2021-02-06	07/02/2021	08/02/2021	09/02/2021	10/02/2021	11/02/2021	12/02/2021
Total imported (Wh)	179797	218726	257726	208695	239250	187483	202447	233641
Total exported (Wh)	0	0	0	0	0	0	0	0
Total exchanged (Wh)	179797	218726	257726	208695	239250	187483	202447	233641
Exchange reduction (Wh)	2191	-16830	-16696	-5351	-16843	466	2692	-16567
Exchange reduction (%)	1.20	-8.34	-6.93	-2.63	-7.57	0	1	-8
Max Peak	12761	13265	13191	13436	12771	11687	12926	11675
Peak reduction (%)	18.2	17.0	19.5	20.6	18.6	18.0	19.7	17.1
Total variability	0.42	0.20	0.09	0.32	0.12	0.37	0.40	0.08
Reduction of variability (%)	30.3	48.0	54.7	36.0	56.2	28.9	23.5	67.9
PED+Bat losses (Wh)	18605	18586	18141	18559	18371	18557	18156	18297
Losses vs exchanged energy (%)	-3.8	-3.7	-3.6	-3.8	-3.3	-4.3	-3.3	-2.9
Total Generation	82460	60620	35280	75940	48670	85510	94560	36720
Total Energy (imported+ generation)	262257	279346	293006	284635	287920	272993	297007	270361
Local Consumption (Total-Exported)	262257	279346	293006	284635	287920	272993	297007	270361
Consumption excluding PED+Bat losses	**243652**	**260760**	**274865**	**266075**	**269549**	**254436**	**278851**	**252064**

Table 10 shows how exported energy has been reduced to zero by scheduling the battery (days 5, 8,10 and 11/2/2021). However, this has a cost due to the operation of power electronics and charge/discharge operation of batteries (PED and battery losses) resulting in an increase of energy demanded in some days (negative exchange reduction) when there is not enough local production. Only the days with enough exceeding production to compensate losses, a reduction on the exchanged energy can be seen.

Table 10 Summary results

GOS (Nu=0.8)		TOTAL (*)	DAILY AVERAGE	AVERAGE ONLY EXP
Total imported (Wh)		1727766	215971	194606
Total exported (Wh)		0	0	0
Total exchanged (Wh)		1727766	215971	194606
Exchange reduction (Wh)		-66937	-8367	0
Exchange reduction (%)	(*)max	1	-4	0
Max Peak	(*)max	13436	12714	12703
Peak reduction (%)	(*)max	20.6	18.6	19.1
Total variability	(*)max	0.42	0.25	0.38
Reduction of variability (%)	(*)max	67.9	43.2	29.7
PED+Bat losses (Wh)		147273	18409	18469
Losses vs exchanged energy (%)	(*)max	-2.9	-3.6	-3.8
Total Generation		519760	64970	84618
Total Energy (imported+ generation)		2247526	280941	279223
Local Consumption (Total-Exported)		2247526	280941	279223
Consumption excluding PED+Bat losses		**2100253**	**262532**	**260754**

Conclusions and remarks

- The schedule provided by the GOS maintains a similar state of charge of the battery at the end of the day. This is important to keep the battery prepared for the next day.
- The GOS avoids exporting energy and uses this to flatten the curve.
- Main contribution to loss reduction is achieved by flattening the curve. This is quantified, in average (Table 10), by reducing the peak around 18% and the variability of the curve in 43%.
- The consumption of the PED and batteries together is around 6.5% of total energy managed (more than 4% is consumed by the PED). This implies increasing the total energy around 4%. This extra energy consumption could be compensated by an increase of local production, or what is the same, an increase of hosting capacity.
- Since the PED and the battery are operative during the whole day, charge/discharge is scheduled to flatten the curve even though there is no production surplus.
- The average energy exchanged during the days with exceeding energy (194kWh) is practically the same with and without GOS, despite the additional consumption introduced by the PED and battery. The difference is that without applying GOS some exchange corresponds to exported energy whereas with the application of GOS the imported energy increases in a similar quantity to compensate PED and battery losses.
- Due to the increase of energy required to run the PED and battery, it is recommended to limit the operation of the GOS only when the excess of PV is enough to compensate this consumption. During the test only days 5,8,10 and 12/02/2021 produces excess of generation (between 5.8-9.6 kWh) and this excess does not compensate the losses in the PED and batteries (18.1 -18.6 kWh).

4.3. Control Indicator 1: Efficiency rate of the PED and the energy storage system

4.3.1. Followed methodology

The objective of this control indicator (CI) is to evaluate the efficiency or power loss of the PED. The PED is built as addition of three electronic power stages. Therefore, three different efficiency coefficients must be calculated for the two isolated DC-DC converters or Dual Active Bridge (DAB) converters and one for the inverter. Considering that it is not expected to obtain a constant parameter, its power losses are evaluated under different PED operating points.

As shown in Figure 12, the power is measured at each battery location, at the grid side, and in DC link.

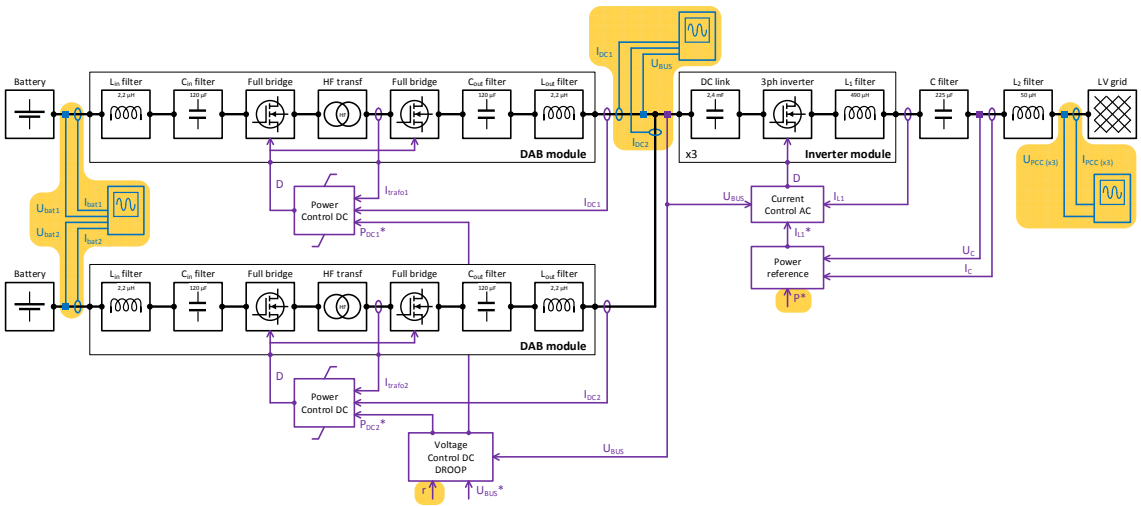

Figure 12 PED measuring scheme

4.3.2.Calculations and results

After collecting data from various scenarios, the different stages (DAB and INVERTER) and the global losses are depicted in Figure 13.

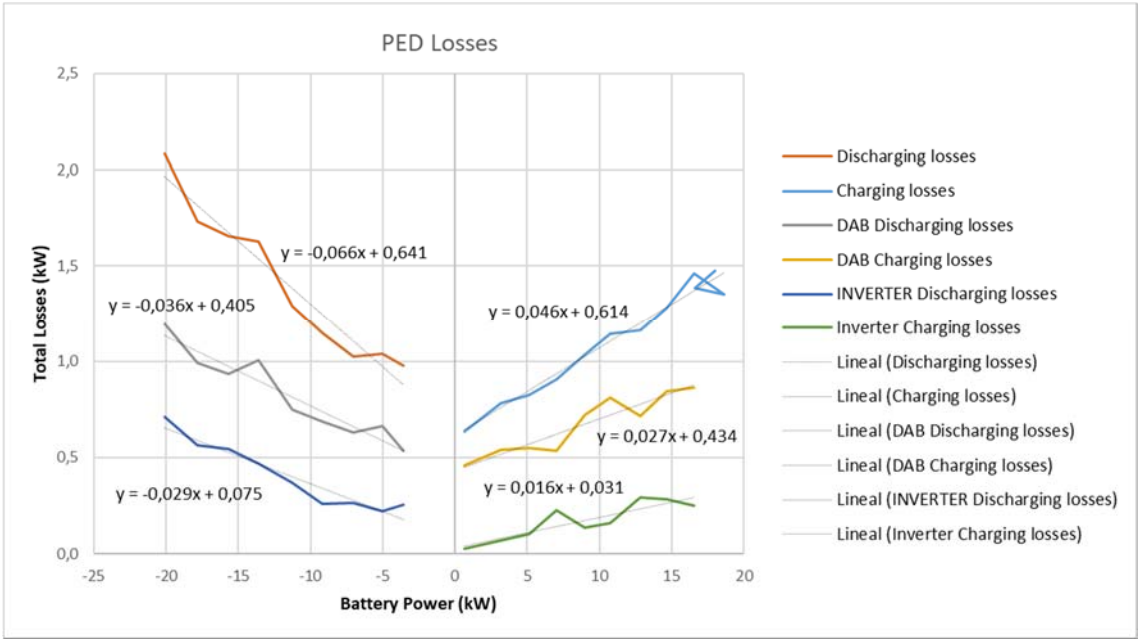

Figure 13 PED losses as a function of the battery power

Then, linearizing experimental values, the losses of the DAB, the inverter, and the PED both when charging and discharging, can be modeled as:

Power losses of the DAB when charging:

$$P_{L\,DAB}(charging) = 0.027 \cdot |P_{BAT}| + 434\,W$$

Power losses of the DAB when discharging:

$$P_{L\,DAB}(discharging) = 0.036 \cdot |P_{BAT}| + 405\,W$$

Power losses of the INVERTER when charging:

$$P_{L\,INV}(charging) = 0.016 \cdot |P_{BAT}| + 31\,W$$

Power losses of the INVERTER when discharging:

$$P_{L\,INV}(discharging) = 0.029 \cdot |P_{BAT}| + 75\,W$$

Power losses of the PED when charging:

$$P_{L\,PED}(charging) = 0.046 \cdot |P_{BAT}| + 614\,W$$

Power losses of the PED when discharging:

$$P_{L\,PED}(discharging) = 0.066 \cdot |P_{BAT}| + 641\,W$$

Therefore, a global efficiency of 95.4% can be assumed when charging and 93.4% when discharging, adding a constant usage of about 600 W. The equivalent efficiency is depicted in Figure 14.

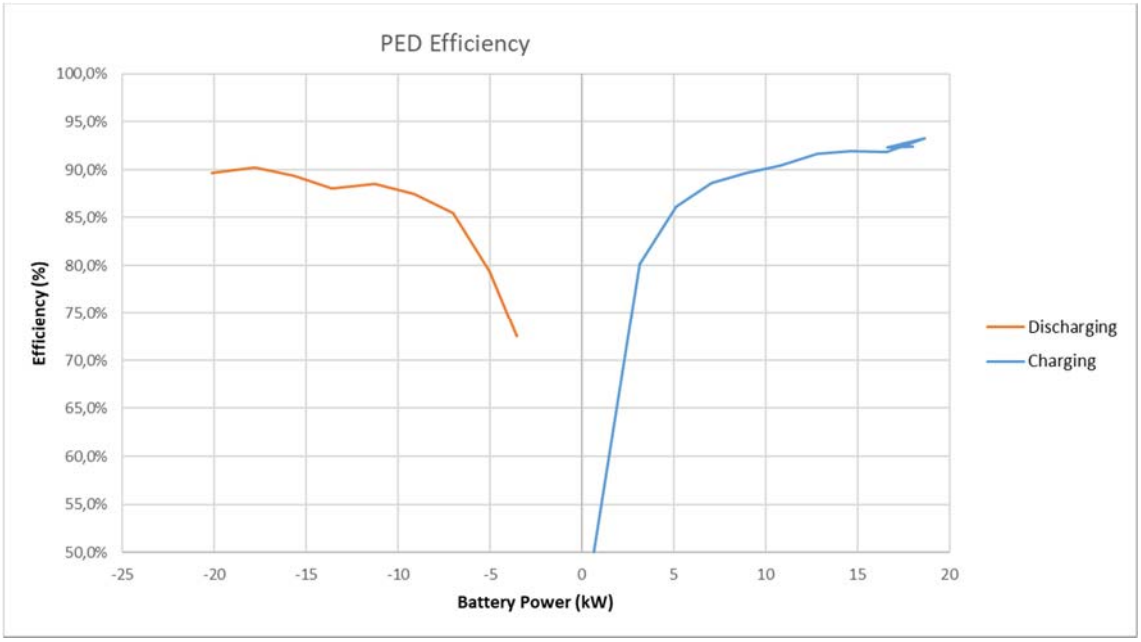

Figure 14 PED efficiency as a function of the battery power

4.4. Test and KPI 3: Increase of DERs hosting capacity in LV network

To protect citizens from electrical outages and problems derived from an excessive and uncontrolled installation of DERs, each country defines and regulates the maximum hosting capacity based on rules-of-thumb criteria. In Spain, the total DG rated power should be lower than the 50% of the transformer rated power, lower than 50% of the thermal limit of the affected feeders and lower than 10% of the short circuit capacity of the point of common coupling (PCC).

These rates of installed capacity are not common in Spanish territory, and in general it is unlikely, nowadays, to have technical issues related to DERs generation. The same applies to the RESOLVD pilot area. The main risks associated to the DERs installation are over-voltages, feeder over-loading, reduction of waveform quality and increase of protection faults.

4.4.1.Followed methodology

The following assumptions are taken:

- The loading limit of the radial network considered depends on the maximum power consumption of the loads located downstream the point considered. This could be related to a physical limit of the feeders.
- Generators do neither generate nor consume reactive power.
- The networks considered are of radial type.
-

4.4.2. Calculations and results

For this KPI calculations both the maximum generated power in the BAU situation and with RESOLVD technology need to be known. The LV distribution network of the two feeders has a gauge section of 240 mm^2 Al, which means a distribution capacity of 400 A. For the calculations, the thermal limit of these will be considered, and therefore the cable capacity is reduced to 330 A. Therefore, at a voltage of 400 V in a three-phase network, an apparent power is calculated as follows:

$$S = V \cdot I \cdot \sqrt{3} = 330\ \text{A} \cdot 400\ \text{V} \cdot \sqrt{3} = 228{,}62\ \text{kVA}$$

Assuming then a power factor of 1, the active power can be deducted as the same value.

$$P = 228{,}62\ \text{kW}$$

Taking into consideration that the distributors only manage 65% of the generation capacity in the same network with respect to the consumption capacity, it is assumed that the network will be able to generate 65% of 228 kVA without RESOLVD, which means 138 kVA. Estabanell has considered a useful capacity of the PED + Batteries of 51 kVA, so the generation capacity in the same network will increase to 189 kVA.

$$S_{WRES} = 138\ \text{kVA}$$

$$S_{RES} = S_{WRES} + 51\ \text{kVA} = 189\ \text{kVA}$$

In this case, the actual maximum generated power without the RESOLVD support is 138 kVA, and with the PED and batteries help this value can go up to 189 kVA, taking into consideration the most limiting capacities of the pilot cables.

Therefore, the change on generated power after the developed technology is placed on site, can be calculated as follows:

$$S\ Change = \frac{S_{RES} - S_{WRES}}{S_{WRES}} = \frac{189\ kVA - 138\ kVA}{138\ kVA} = 36{,}95\%$$

Finally, if the calculated value of power is multiplied by the percentage of change of generated power calculated before, the following value is obtained:

$$KPI3 = 228{,}62\ \text{kW} \cdot 36{,}95\% = 84{,}45\ \text{kW}$$

4.5. Test and KPI 4: Reduction of DSO investment

4.5.1.Followed methodology

This KPI is independent from any real tests of the technology, and it consists of a simple calculation. First, the problems tackled by RESOLVD are considered:

- Congestion issues
- Over/undervoltage issues
- Poor power quality upstream the PED
- Power interruption, making grid reconfiguration necessary
- Power interruption, making island-mode necessary
- Etc.

For each of these problems, a RESOLVD and a BAU solution are identified. The followed steps are:

- Collect input data
- Calculate KPI-05
- Perform sensibility analysis

4.5.2. Calculations and results

First, a traditional infrastructure investment will be considered, consisting of a LV line together with a transformer. If an average distance of 100 meters is assumed, and a cost of the line per meter is known to be 159,07 €:

$$C_{LVnetwork} = 100m \cdot 159{,}07€ = 1.590{,}7\ €$$

The average cost of the transformer for this case, is 24.000 €. Therefore, the total cost of the traditional infrastructure is the addition of the cost of the line together with the cost of the transformer.

$$C_{TotTrad} = 1.590{,}7\ € + 24.000\ € = 25.590{,}7\ €$$

With this, it can be stated the minimum cost of the RESOLVD technology, considering the PED and the batteries, should be of 25.590 €, for the DSO investment to be neutral. Nevertheless, the market price for a 75 kW PED is already 35.000 €, and the average cost of the combination of lithium-ion and lead acid batteries is 137 € per kWh. The total cost of the batteries set up for the RESOLVD case is then:

$$C_{Bat} = 137\frac{€}{\text{kWh}} \cdot 48\ kWh = 6.576\ €$$

Consequently, the total cost of the whole system is the addition of the PED market price together with the cost of the batteries:

$$C_{TotRes} = 35.000\ € + 6{,}576€ = 41.576\ €$$

With these two total cost of the traditional and the RESOLVD set ups, the DSO investment variation can then be calculated as follows:

$$Investment\ variation = \frac{C_{TotTrad}}{C_{TotRes}} = \frac{25.590{,}7€}{41.576€} \cdot 100\ = 61{,}55\%$$

$$KPI3 = C_{TotRes} - C_{TotTrad} = 41.576€ - 25.590{,}7€ = -15.985{,}3\ €$$

The actual technology is then 61,55% more expensive compared with a traditional investment. It is worth mentioning that this should be further analysed taking into consideration the reduction of the maintenance costs that the PED and batteries will provide in the long term, in order to analyse the profitability of this initial investment.

4.6. CI 02: DSO operation expenditures with respect to the BAU solutions

This control indicator aims at monitoring the operational costs (OPEX) associated to the RESOLVD technology and make sure they do not overcome the operational costs of a BAU solution. In order to compare OPEX of RESOLVD and the ones of a BAU solution, the same assumption as for the KPI-05 needs to be made: if no technology exists, which can bring the same value of RESOLVD, the more similar device or solution will be considered.

When talking about the specific case of the Spanish pilot, it is worth mentioning that before 2021 the remuneration for the operation and maintenance, was stated in the Spanish rule in force until RD 1048/2013 + Order IET / 2660/2015. This differentiates between O&M of electrical assets (which is remunerated by unit value) and O&M of non-electrical assets (which is remunerated by invoice). The O&M amount of electrical assets ranges from 3% to 5% of the unit investment reference value.

In this case taking as a reference an investment value of 57.000 € as a usual new building of network assets at LV level including a secondary substation, the O&M cost was:

$$O\&M_{before21} = 57.000\ € \cdot 4\% = 2.280\ €/\text{year}$$

Nevertheless, the new Spanish regulation (Circular 6/2019) which is already in fully force, eliminates the O&M remuneration directly linked to electrical assets and sets the remuneration for O&M, together with other concepts, within a new term called COMGES (Component Manageable of the Expense). This term is no longer indexed to the units of electrical assets owned and built. This is a type of salary, set based on the distribution history of each distributor and reviewed annually downwards, as it is to encourage the efficiency of the distributor.

4.7. Test and KPI 5: Percentage improvement in line voltage profiles with power injection and consumption

One of the objectives of this project is to control the voltage level in LV distribution network. Due to an increasing presence of distributed generation, the voltage is becoming more difficult to control and over/undervoltage issues are more and more frequent. Through the power electronics technology it is possible to exchange power with the grid, thus regulating the voltage level when a voltage variation is detected or forecasted.

4.7.1.Followed methodology

This test aims at calculating the voltage per power gain through the grid equivalent resistance and inductance. Ideally, to perform the test the PED should be connected alone in the distribution system, however, the consumers cannot be switched off without sacrificing their supply. Therefore, the test can be performed when the consumption and the generation is almost null or have an opposite pattern that the test will perform (e.g. inject power to the grid when the consumption is higher than generation, or extract power from the grid when the generation is higher than consumption).

4.7.2. Calculations and results

For the testing day, the switchgear configuration is changed from standard [101] to [110], having the PED at the end of the radial line and permitting the increase or decrease of the voltage levels by injecting or consuming power, respectively. The power and voltage data was collected and is represented graphically in this section's Figures. The green line represents the values collected by PQM 2, located at the beginning of the line, right after the substation SS528, and the red line represents values collected by PQM 9, located at the end of the same line, right where the PED is connected. It is important to note that the equivalent voltage of the grid is not constant, but it is assumed that the variations are small. In addition, the upper grid configuration can be modified during the operation varying the grid parameters. However, it is assumed that the grid parameters will remain similar.

As it can be seen in Figure 15, during the morning hours different values of active power were injected and consumed by the PED, in equally long intervals and keeping a steady increase between them, always reaching a maximum value of 5kW in both PED states of consumption and generation.

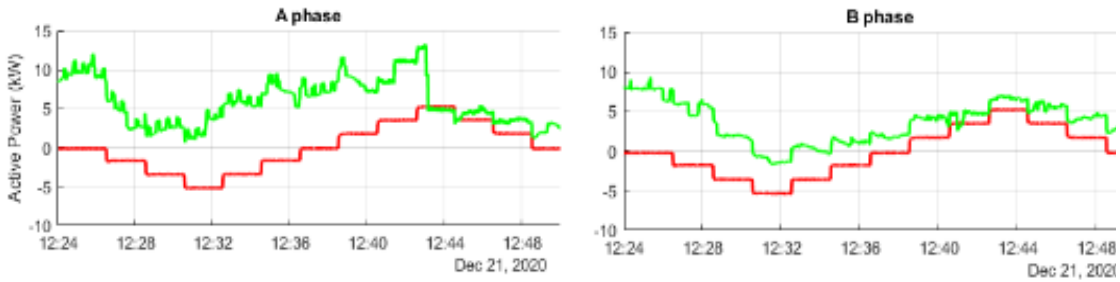

Figure 15 Active power [kW] of phase A, B and C during test of KPI 5

In the following image, Figure 16, the effect of these power variations on the voltage level can be seen, both at the beginning and at the end of the line. It is noticeable that the voltage measured by PQM 9, differs from the one measured by PQM 2, being slightly higher during the power injection time of the PED, and lower during the power consumption time of the PED.

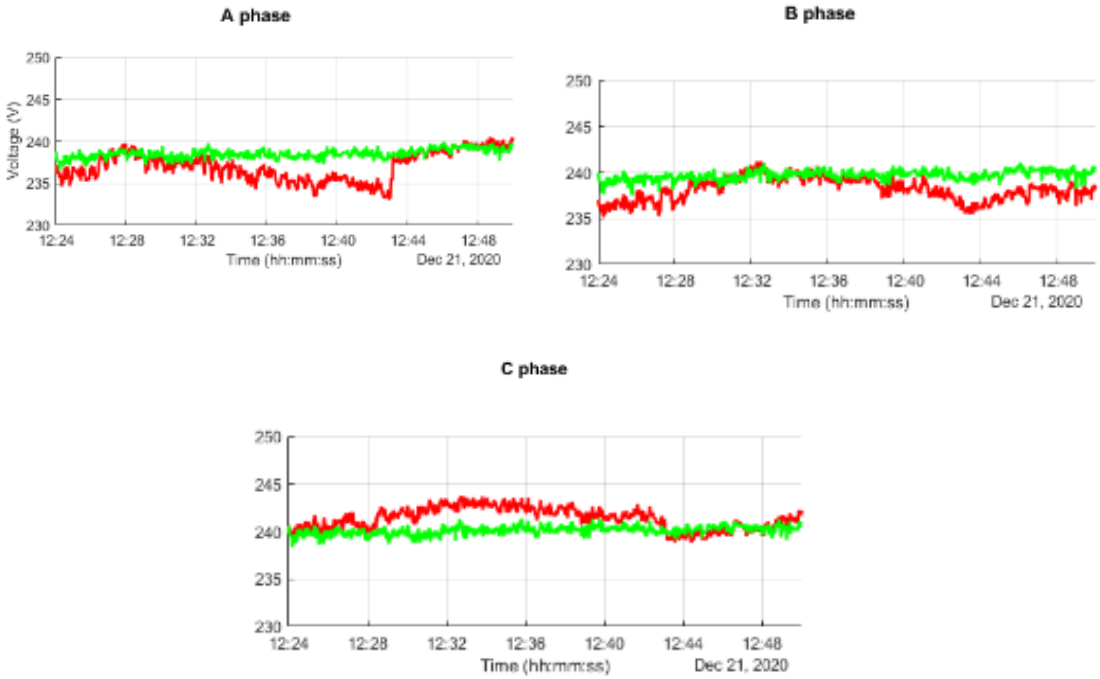

Figure 16 Voltage [V] of phase A, B and C during test of KPI 5

This difference of voltage can be seen more legible when plotted as the subtraction of the two values during the time of the test. The graph outline for the three phases follows the same pattern, with different values as already discussed, being the tension at the end of the line higher when the PED is set to generation mode, and lower when this is set to consumption mode.

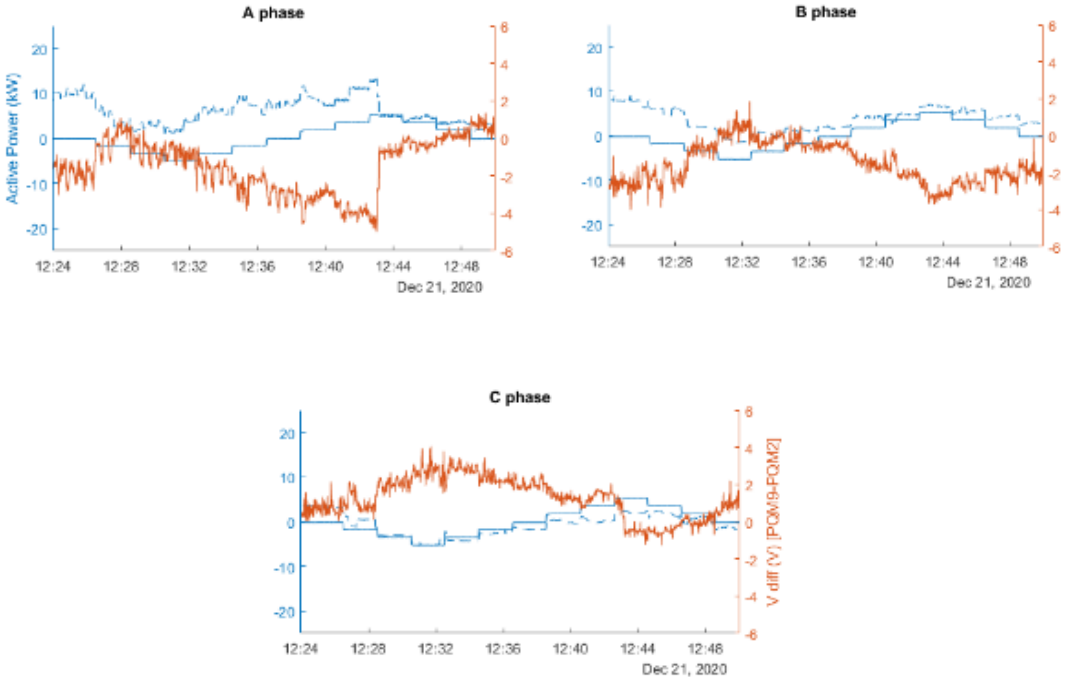

Figure 17 Voltage difference [V] over active power of phase A, B and C during test of KPI 5

With this difference plotted and quantified, it is possible to calculate the line equivalent resistance and inductance. The following equation allows to determine the grid parameters through the input data (voltage, active and reactive power). Assuming that V is approximately (1 pu), then it is possible to estimate the rest of the parameters.

$$V_{PQM2} - V_{PQM9} = \frac{R * P + Q * X}{V^2}$$

$$R = 0{,}08\Omega$$

$$L = 160\ \mu H$$

$$X = 0{,}05\Omega$$

$$Z = 0{,}08 + j0{,}05$$

Using these calculated values, it is possible to plot together both the measured and the calculated values of the voltage difference between the beginning and the end of the line. As it can be seen in Figure 18, the two values for the three phases are quite similar.

A phase B phase

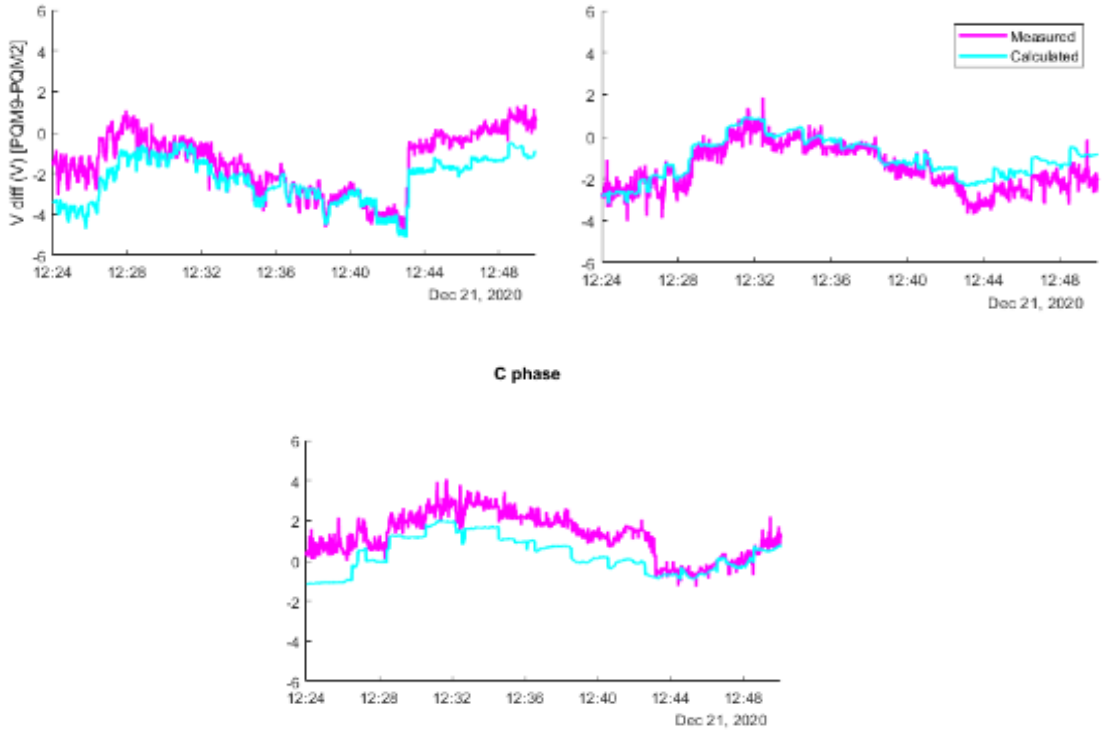

Figure 18 Measured and calculated voltage difference [V] of phase A, B and C during test of KPI 5

The same analysis can be done with the reactive power. The same methodology was followed, injecting and consuming different values of reactive power, during intervals of equal time, and equally incremented. These values reached a maximum of 20 kVA, both when in load and in generation mode, when the PED is considered inductive and capacitive load, respectively. The following graphs show how in this case, both PQM 2 and PQM 9 see the same pattern of injection and consumption of reactive power.

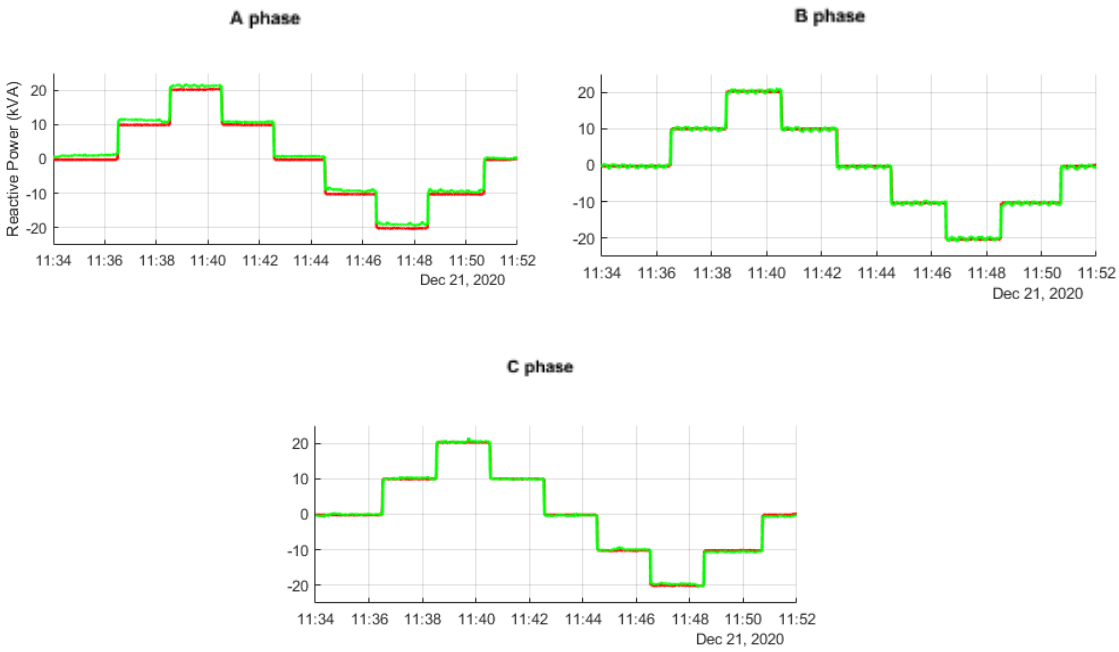

Figure 19 Reactive power [kW] of phase A, B and C during test of KPI 5

In the following image, Figure 20, the effect of these power variations on the voltage level can be seen, both at the beginning and at the end of the line. It is noticeable that the voltage measured by PQM 9, differs from the one measured by PQM 2, being again slightly higher during the power injection time of the PED, and lower during the power consumption time of the PED.

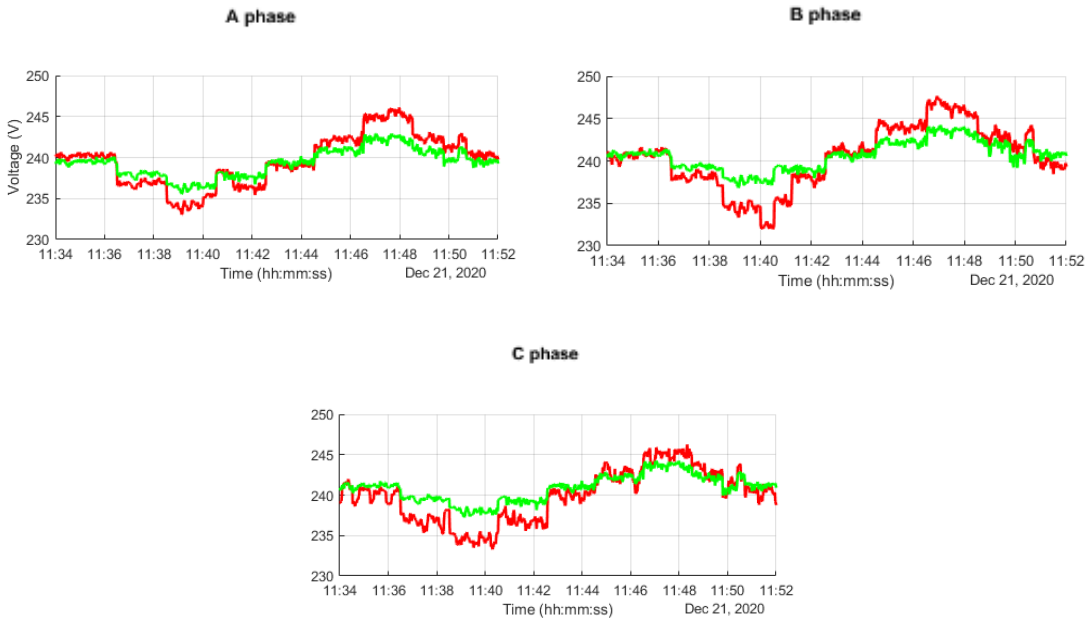

Figure 20 Voltage [V] of phase A, B and C during test of KPI 5

Once again, it is possible to see voltage difference more legible when plotted as the subtraction of the two values during the time of the test. The graph outline for the three phases follows the same pattern, with different values as already discussed, being the tension at the end of the line higher when the PED is set to generation mode, and lower when this is set to consumption mode.

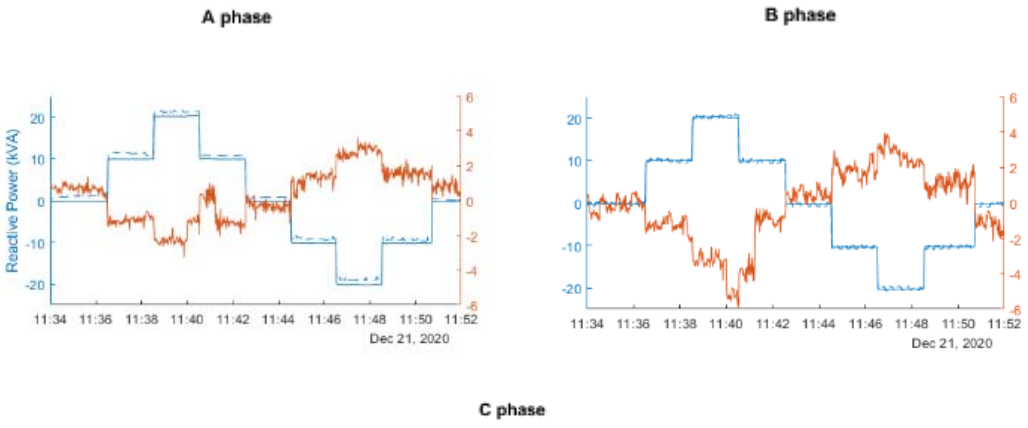

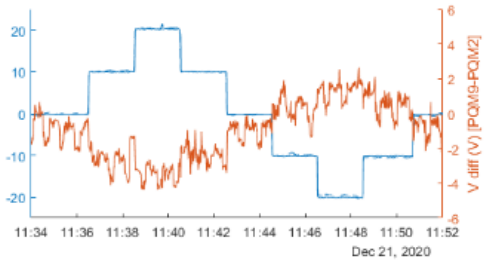

Figure 21 Voltage difference [V] over reactive power of phase A, B and C during test of KPI 5

Using the previously calculated values, it is possible to plot together both the measured and the calculated values of the voltage difference between the beginning and the end of the line. As it can be seen in Figure 22, the two values for the three phases are quite similar.

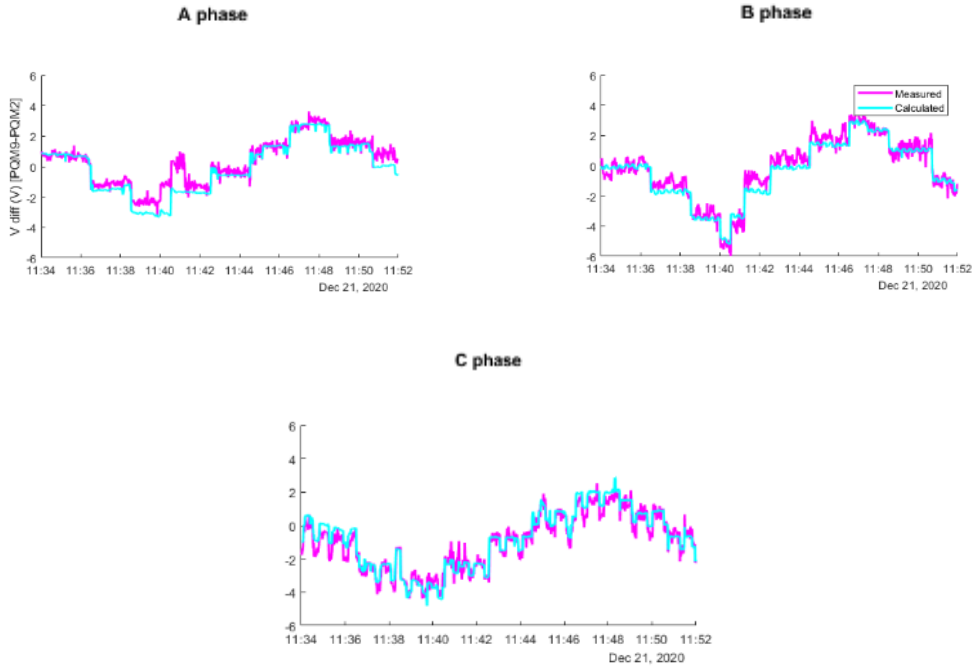

Figure 22 Measured and calculated voltage difference [V] of phase A, B and C during test of KPI 5

4.8. Test and KPI 6: Rate of prevented critical events in the LV grid due to forecasting and remote control of grid actuators

In the pilot site there was no technology devoted to predicting a critical event (congestions / over/sub voltages) previously installed to be used for comparison. Moreover, the expected situations at the beginning of the project changed because largest consumer in the pilot area closed the activity resulting in a reduction of the demand and consequently reducing the stress on the circuits under test.

Consequently, it is not possible either to compare the added value of RESOLVD solution w.r.t existing one or analysing the response of the system to real events. Thus, the performance of this service has been measured in terms of effectiveness and considering artificially created

congestions. Thus, the event forecasting capability has been evaluated by downsizing the ampacity of a line segment and changing the configuration of the grid to get the maximum current flowing through this segment. Once a possible congestion is forecasted, the Grid operation scheduler is invoked to propose changes in the grid configuration that avoids the congestion.

4.8.1.Followed methodology

This test aims at evaluating the capability to forecast and avoid possible critical events. The basic procedure for critical event avoidance consists in the following steps:

1- Day ahead forecast generation and demand at the bus level: Since SM data comes with hourly resolution, this will be also the resolution of forecasting.
2- Critical event forecasting: Launch a power flow simulation for every hour in the day ahead forecasting and get possible critical events.
3- In case of possible critical events forecasted the application launches a grid operation scheduling (GOS) aiming to reconfigure the grid to avoid such events with the minimum number of switching operations.

Test scenario

Currently the lines in the pilot are oversized with respect to the demand and generation it hosts, and consequently real critical events are not expected. Given this situation, critical events have been generated artificially by downsizing the ampacity parameter of specific line in the pilot. This allows creating artificially critical events associated to a congestion in the specified line segment without affecting the normal operation of the grid. At the same time, this strategy reduces uncertainty during the evaluation since the real location of the supposed congestion is known.

The proposed test scenario is represented in the Figure 23. The red segment represents the relative position of the weakest part of the grid with the selected configuration set at [011] with all the load and generation connected to the same substation SS-B (SS030). The segment labelled as 155722 corresponds to the real segment which ampacity has been substantially reduced to, in somehow, simulate a thinner line. Switchgear configuration code corresponds to the triplet (SG1, SG3, SG2) and values represent 1/0 (closed/open).

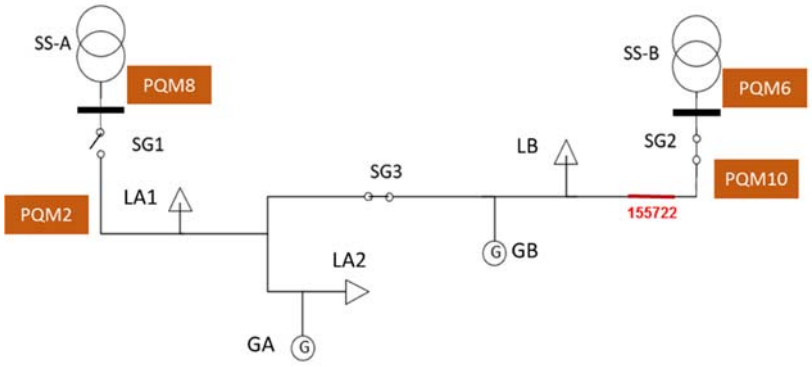

Figure 23 Grid configuration and relative location of the artificially created weak segment

The Power Quality Monitors (PQM) installed at the headers (PQM2 and PQM10) have been used to gather data during the test that has been used for validation.

Test Description: Basic parameters and set up

Critical Event Forecasting has been launched for two different grid configurations in order to check how these differences produce an increase of current that could be associated to a congestion:

- Test 1: normal exploitation (101) when no critical events are expected
- Test 2: grid configuration set to 011 (all the load fed by the same substation). Increment of load is expected to create a congestion at the peak hour.

Basic test data:

- Test date: 16/12/2020
- Downsized segment:
  - Real location: segment '155722' (SS030)
  - Current threshold (ampacity): 13A.
- Grid Configuration:
  - Test 1: 101 (normal configuration: two SS)
  - Test 2: 011 (All the load fed by the same substation SS-B (33030)
- CEPA: It is launched the day before, and calls the following basic services:
  - Energy forecasting (requires previous training of models)
  - Critical event forecasting
  - Grid operation Scheduling (only SG operation) if necessary (CEF detected)
  - Switchgear operation: manually executed.
- Data gathering: PQM10.

4.8.2. Results and discussion

As an outcome of launching the Critical Event Prevention Application (CEPA) for both tests pointed in the previous subsection for the same date (16/12/2020), the Critical events listed in Table 11 were obtained (no critical event in Test 1 and two events for Test 2).

Table 11 Critical Events forecasted in the Test 1 and Test 2

Test 1 (Grid Config 101)	Test 2 (Grid Config 011)
-	TSini: "2020-12-16T09:00:00", TSend: "2020-12-16T10:00:00", Type": "congestion", AffectedID": "155722", Values": 15.19 Deviation": 16.92
	TSini: "2020-12-16T18:00:00", TSend: "2020-12-16T23:00:00", Type: "congestion", AffectedID: "155722", Values: [15.1, 18.91, 21.29, 18.46, 16.78 , Deviation: 16.22, 45.56, 63.91, 42.07, 29.2

Together with the CEF (Test 2), the applications return a solution provided by the Grid operation scheduler (GOS). Since the GOS looks for a solution with the minimum number of switching operations, the solution it returns is quite trivial: return to the standard position at the first hour and do not change from that configuration. The SG schedule can be seen in Table 12.

Table 12 Schedule to solve the congestions forecasted in the Test 2

	1	2	3	4	5	6	7	8	9	10	11	12
SG1	0	1	1	1	1	1	1	1	1	1	1	1
SG2	1	0	0	0	0	0	0	0	0	0	0	0
SG3	1	1	1	1	1	1	1	1	1	1	1	1
	13	**14**	**15**	**16**	**17**	**18**	**19**	**20**	**21**	**22**	**23**	**0**
SG1	1	1	1	1	1	1	1	1	1	1	1	1
SG2	0	0	0	0	0	0	0	0	0	0	0	0
SG3	1	1	1	1	1	1	1	1	1	1	1	1

The effect of changing the configuration from (011) to (110) is evident. The current from SS-B (SS030) is reduced to zero, since all the consumption is moved to SS-A avoiding any possible event in the critical segment. However, this change in the configuration requires passing through an intermediate state (011→ 111 →110) associated, the ring configuration. In the pilot site, the grid configuration produces an overcurrent (see current evolution for different states in PQM 10 in Figure 24) due to the difference of voltages among substations (voltage in SS-A is boosted around 10V higher than SS-B) before the interconnection (See figures PQM1:V and PQM10:V in Figure 21). This voltage difference forces a power flow from SS-A to SS-B when configuration [111] is set.

Based on this issue, it is important to remark that the grid operation in the pilot can be used to solve long congestions but when this reconfiguration requires passing through the state [111] it is important to know that this will produce a substation increase of current to compensate the potential difference between substations.

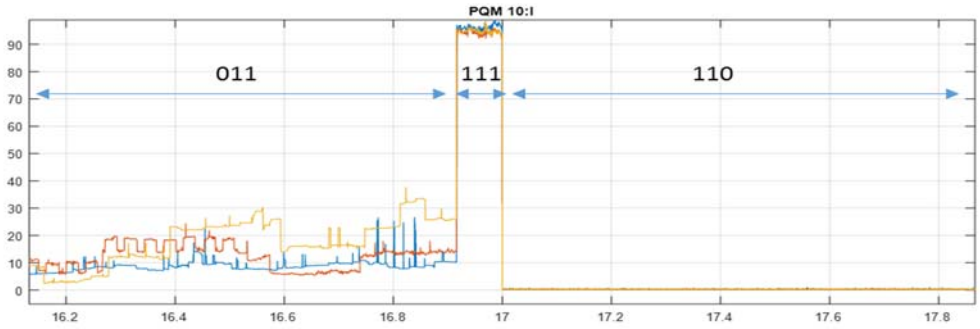

Figure 24 Transition from grid configuration 011 to 110

Performance indicators

Due to the impossibility to create real events in the pilot, performance has been reduced to evaluate the tool working in the integrated environment consuming real data. The evaluation has consisted in analysing the consistency of outcomes for different situations according to the real context that the pilot offers.

Additional remarks and observations

During the tests, some differences in the voltage profiles returned by the power flow have been identified. These were due to two circumstances: the different boosting of secondary substations that result in a difference of 10 volts approximately (previously discussed) between both and the existence of adjacent lines in the secondary substations not considered when modelling. Figure

25 represent voltage and currents per phase at the secondary substation (SS030: PQM6 and SS528: PQM8) and the pilot line (SS030: PQM10 and SS528: PQM2) respectively.

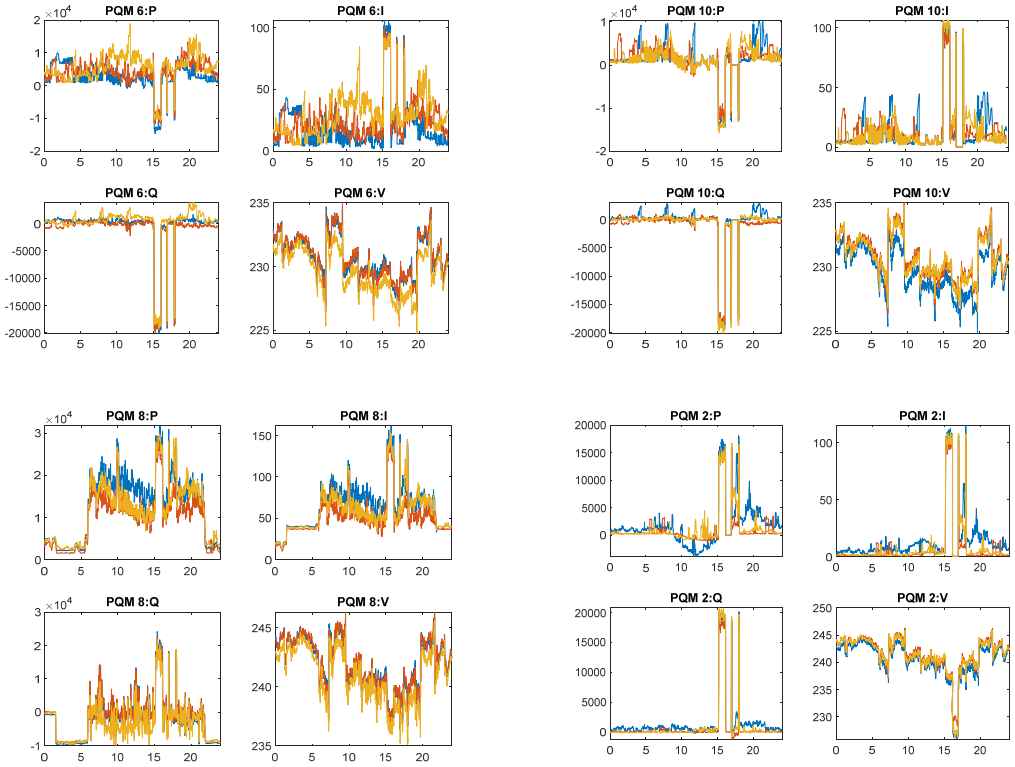

Figure 25 Voltages and Currents and SS and pilot lien during the KPI6 test

The results from the tests carried out have permitted to adjust voltage variations among secondary substations due to consumption from other lines not considered previously:

- SS528 (250kVA) is loaded with an industry and some residential customers in adjacent lines for a connected power around 70kW.
- SS030 (530kVA) is loaded with 30kW in adjacent lines.

Average power profiles from PQM8 (SS528) and PQM6 (SS030) have been used to adjust these loads in the respective SS considering for both a power factor of 0.8.

4.9. Test and KPI 7: Quality of online event detection in LV grid

The purpose of this KPI is to analyse the capability of the Fault Detection Application to detect faults in the low voltage distribution systems. A fault can be defined as a deviation of voltages and/or currents from nominal values or states that could result in an unsafe, or undesired, operation of the system or a part of it.

In order to get information from tests performed in the real scenario of the pilot, we proceed to generate artificially situations that could be associated with abnormal operation of the grid and resulting in a variation of currents in a magnitude representative enough for a faulty situation but not affecting the continuity of supply.

4.9.1. Followed methodology

To evaluate KPI7 in the real environment the main guidelines pointed in D5.1 have been followed. However, instead of creating artificial faults by modifying data recorded by PMUs, a more realistic

scenario has been recreated and variations have been provoked by operating switchgear to create an overloading situation in the grid.

Test scenario

The radial configuration of the grid has been considered as the normal test configuration for the pilot grid. Since the configuration can be modified by operating three possible switchgears (labelled as SG1, SG2, SG3 in Figure 26a), this results in three possible configurations considered as normal (listed in the Table 13). And the ring configuration (111) has been considered as the faulty situation to detect.

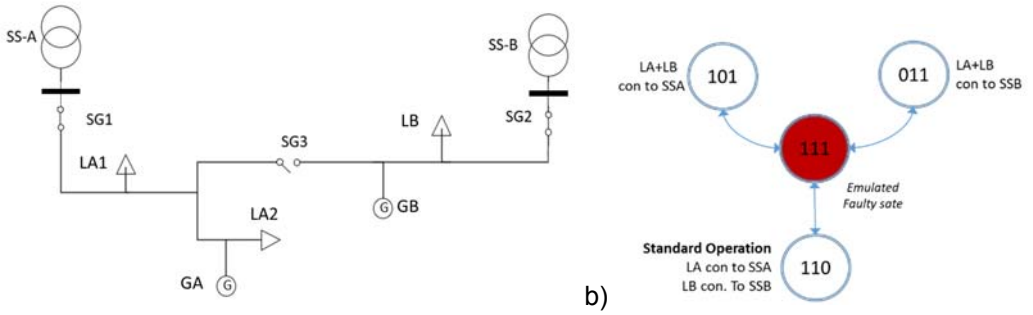

Figure 26 Pilot grid schema and location of switchgears (a) and related states (b)

Table 13 Grid configuration of normal and faulty situations during the test

Grid Configuration		Number of models	Variables in the model
011	All the prosumers fed by SSB	1	3 Ph Currents
101	Two feeders: standard test configuration	2	3 Ph Currents
110	All the prosumers fed by SSB	1	3 Ph Currents
111	Ring configuration: considered faulty for this test	-	

Thus, the objective of the test is to evaluate the capability of the fault model to detect a change in the configuration by analyzing measurements gathered by PMUs in the extreme of the lines.

Set up

The FDA module has two operation modes: training and monitoring. Fault detection is performed in the second mode by continuously evaluating registers acquired by the PMUs and supplied through the ESB to the Fault Detection Application. Before this continuous operation, the module requires training of the models to be used as reference. In the test three configurations have been considered normal, so training for every model has been performed with data collected during a complete day previous to the test. Thus, data collected the dates 20, 22 and 25 of January (Wednesday, Friday, and Monday respectively) have been used to train the reference models for configurations (110, 011 and 101) respectively.

During monitoring there is a tradeoff between the frequency of invocations and the number of samples (time window) being evaluated at every invocation. However, the results of the detection are associated to every sample; so, this has only implications on the time when the fault is informed but not in the accuracy of the detection. Since a different model is used as reference for the different configuration considered normal (101, 110 and 011), this configuration is communicated together with every dataset being evaluated. Again, delays in communicating the update in the grid configuration status can result in both errors and/or delays in the detection, associated to the use of a wrong reference model.

The data used in the tests was collected by PMU 3 and PMU 4 installed at the substation after the SGs.

Test description: basic parameters

- Test time: 26/01/2021, from 9AM to 19PM

- Grid Configuration

  Update time: 1 min

  Test sequence: A sequence of variations in the grid configuration from normal states to the faulty states have been performed by acting directly on the switchgears (See Figure 27)

- PMU sampling time: 1 sec

- FDA invocation (monitoring window)

  Frequency: every 5 minutes

  Samples in the Time Window: ~ 300 (sampling time 1 sec)

-Response time of the FDA module:

  Monitoring mode: 20-35 sec.

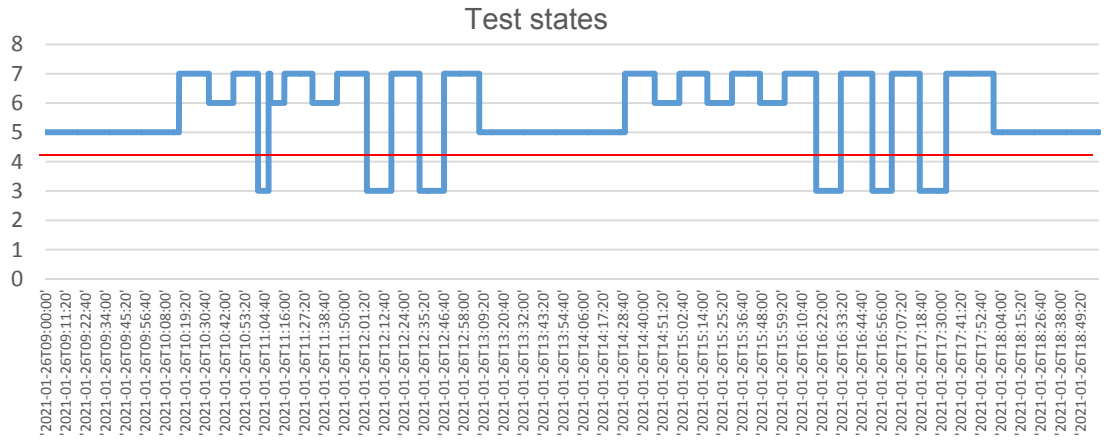

Figure 27 Evolution of states during the test (7: 111-faulty-, 6: 110, 5:101, 3:011) executed between 09AM and 19PM (26/02/2021)

Performance indicators

The outputs of the fault detection module during the test have been summarized in a confusion matrix to discriminate among samples correctly and wrongly classified as faults.

Table 14 Confusion matrix

		Real Fault	
		True	False
Detected fault	True	True positive (TP)	False positive (FP)
	False	False negative (FN)	True negative (TN)

Then, the following performance Indicators have been computed, according to D5.1:

Accuracy: Ratio of correctly predicted events (faults and normal states) over total of samples

$$Accuracy = \frac{TP + TN}{TP + FP + TN + FN}$$

Precision: Ratio of correctly detected faults over total of predicted faults.

$$Precision = \frac{TP}{TP + FP}$$

False negative rate (**Missed detection rate**): Ratio of not detected events (wrongly predicted as normal) over all the samples that are really faults.

$$FNR = \frac{FN}{FN + TP}$$

False discovery rate (**False Alarm rate**): Ratio of wrongly detected faults over all the samples predicted as faulty.

$$FDR = \frac{FP}{FP + TP}$$

Detection and information time

For the estimation of the detection time, it is assumed that data is correctly dated by the PMUs and the same time reference is used for all the subsystems.

Under this assumption the time required by the fault detection module is 0, since the computation time is negligible wrt to the sampling time **(T_S)** (1 sec).

However, some delays in the complete operation of the systems are important for the overall performance of the module:

- **Grid information time (T_G)**: time between a grid change in the configuration and informing the FDA module. In the test this has been 1 minute
- **Monitoring window (T_M)**: that is the frequency (period) of invoking the FDA module. During the test this was 5 minutes.
- **FDA module response time** (T_R): 20-35 sec.

Since a fault can occur inside the monitoring window, a delay between the detection and informing on that detection can occur, even though the FDA module informs about the exact time instant of the fault. This is bounded by the duration of the monitoring window.

Additionally, it has been observed that the delay in getting the right grid configuration can produce false alarms, but it does not seem to be a cause of miss detection, so in principle it does not introduce a significant delay.

The maximum delay in informing of a fault is upper bounded by: **T_G+$T_{M+}$$T_R$**

Execution

Every time the grid configuration is changed this is informed by the SCADA and it used to select the appropriate reference model for every configuration. Since mode 111 has been considered as faulty, informing about that configuration was skipped remaining the last known configuration. Figure 28 (up) shows the model being used at every time instant (orange) wrt the real state of the grid (7: 111: faulty state, 3:011, 5:101 and 6:110 the normal states. And the plot in the bottom depicts the evaluation for every PMU (blue dotted and solid lines) and the final decision (black asterisk).

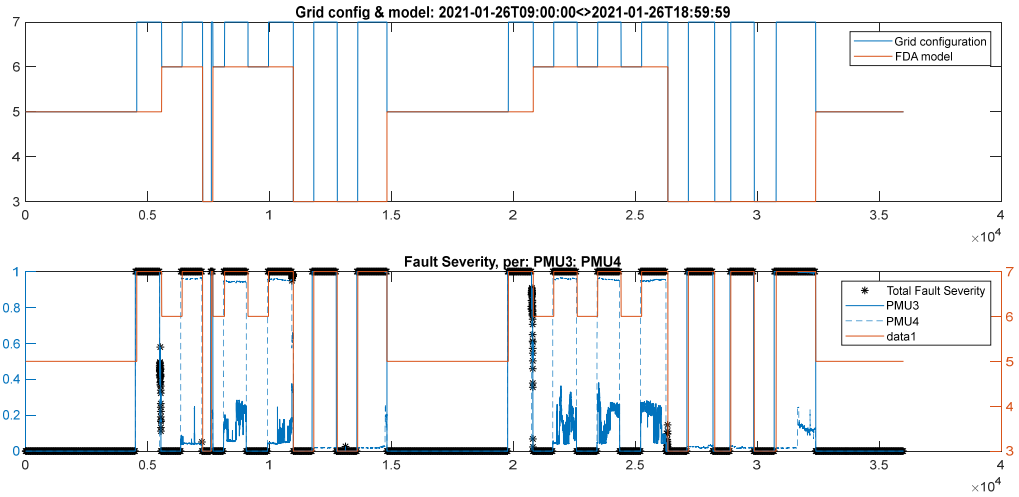

Figure 28 A summary of these decisions according to the real state informed is summarised in the following confusion matrix for a total of 36000 time instants (10h) evaluated during the 26 of January 2021.

A summary of these decisions according to the real state informed is summarised in the following confusion matrix for a total of 36000 time instants (10h) evaluated during the 26 of January 2021. A decision threshold of 0.5 in the severity indicator has been used to decide or not about the existence of a fault.

Table 15 Confusion matrix from the test

		Real Fault		
		True	False	Total
Detected fault	True	12842	1026	13868
	False	0	22132	22132
	Total	12842	23158	36000

4.9.2. Calculations and results

Data from the previous confusion matrix has been used to compute the performance indicators:

$$Accuracy = \frac{TP+TN}{TP+FP+TN+FN} = \quad 0.9715\ (97.1\%)$$

$$Precision = \frac{TP}{TP+FP} = \quad 0.9260\ (92.6\%)$$

$$FNR = \frac{FN}{FN+TP} = \quad 0\ (0\%)$$

$$FDR = \frac{FP}{FP+TP} = 0.0443\ (4.39\%)$$

Effect of delays in informing the real grid configuration status

The delay in informing the grid configuration can produce a loss of performance due to the use of wrong reference model. Figure 29 illustrates this situation, where a sudden reduction of currents in the instant 5500 corresponds to the recovery of a normal state. This change is informed after 81 seconds (grid configuration changes to state 6:110) so the reference model remains the last known (5:101) producing lower performance in the detection (severity is reduced rapidly to 50% but still is considered an abnormal operation and informing of a possible fault when does not

apply).

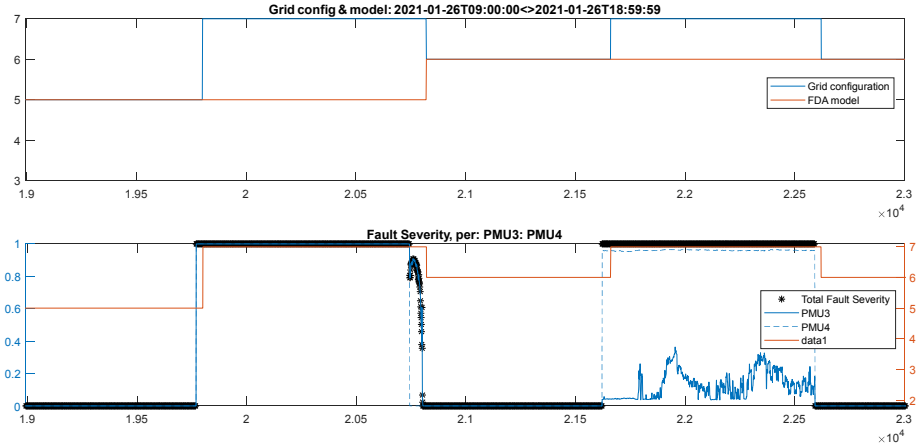

Figure 29 Zoom of previous figure showing delays between detections and informing SG status

Correction of performance indicators to avoid delayed information on grid status:

A more detailed analysis of the detection showed that when a change in the grid configuration was applied, the information system introduced a delay that affected the performance of the detection during those transitions. In order to decouple FDA performance from this delay a correction has introduced. Table 16 summarises the performance for all the transitions incurred during the test. The arrow on the left indicates transition from a normal state to a faulty state (↑) and from the faulty state to a normal state (↓). The following columns informs about the difference between the real state and the informed state and the period when this difference happens.

For these time instants reduced confusion matrix has been filled in order to analyse a possible impact of the use of a wrong model for the fault detection during these transitions. The conclusions for every transition are summarised in the observation's column.

Table 16 Evaluation of transitions and effect of delay in informing the grid status

							Confussion matrix				
	Real grid State	Last state informed	Model used	Sample ini (sec)	Sample end (sec)		TP	FP	TN	FN	Observations
↑	7	5	5	4503	4560		57				No impact
↓	6	(7)	5	5499	5543				44		Wrong model
↑	7	6	6	6366	6420		54				No impact
↓	3	(7)	6	7230	7260				30		Wrong model 6 (3): TN
↑	7	3	3	7588	7620		9	24			No impact
↓	6	(7)	3	7622	7680			58			Wrong model: 3 (6): FP
↑	6	(7)	6	8123	8160		37				No impact
↓	6	(7)	6	9049	9121				72		No impact
↑	7	6	6	9927	9960		33				No impact
↓	3	(7)	6	10921	10980			59			Wrong model: 6(3) : FP
↑	7	3	3	11749	11820		71				No impact
↓	3	(7)	3	12742	12781				39		No impact
↑	7	3	3	13585	13620		35				No impact
↓	5	(7)	3	14740	14820				80		Wrong model: 3(5): TN
↑	7	3	3	19770	19800		30				No impact
↓	6	(7)	3	20743	20822			55	24		Wrong model 3(6): FP, TN
↑	7	6	6	21622	21660		38				No impact
↓	6	(7)	6	22592	22620				28		No impact
↑	7	6	6	23431	23460		29				No impact
↓	6	(7)	6	24337	24422				85		No impact
↑	6	(7)	6	25222	25260		38				No impact
↓	3	(7)	6	26259	26340				81		Wrong model: 6(3) : TN
↑	7	3	3	27121	27180		59				No impact
↓	3	(7)	3	29880	29887				7		No impact
↑	7	3	3	30699	30780		81				No impact
↓	5? (*)	(7)	3	31620	32400				780		Unknown real status (discard)
	(*) Unknown state					**Totals**	**571**	**196**	**1270**	**0**	
					Due to wrong models		**0**	**172**	**995**	**0**	

From this analysis we considered it convenient to recalculate the KPIs in order to isolate the performance of the FDA module from this delay in informing the real status (and consequently the correct model to be used as a reference). Thus, a total of 1167 (172 FP and 1270 TN) time instants (over 36000) have been eliminated from the previous confusion matrix resulting in a total of 34833 time instants for the new study. The following values have been obtained (second row).

Table 17 Performance indicators for KPI6

	Accuracy	Precision	Missed Detections	False alarms
FDA with wrong models	97.1%	92.6%	0%	4.3%
FDA without wrong models	97.5%	93.7%	0%	3.8%

Results and conclusions

The FDA module has an accuracy of 97.5% and precision of 93.7%, for the selected configuration no missed detection have been appeared and the ratio of false alarms is less than 4%.

Some additional conclusions can be derived from the test in the real scenario.

- The method does not require training with previous faults. Only the normal operation modes require training, which makes the method easily adjustable to different operation conditions. This has been validated by allowing the grid to operate in 3 different configurations considered as normal.
- The method exploits statistical redundancy in the data gathered by instruments. For the test two PMUs have been used; however, the module is prepared to manage many PMUs (or other kind of instruments) installed in the grid (same or different voltage levels); being the results general enough and the method scalable to other grids with major complexity.
- Delays in detection are insignificant. However, since a fault can occur inside the monitoring window, despite the FDA module informs about the exact time instant of the fault, a delay between the detection and informing on that detection can occur and this is bounded by the duration of the monitoring window.
- The delay in getting the right grid configuration can produce false alarms, but it does not seem to be a cause of missed detection.
- Data sets contained in every monitoring window were expected to contain 300 samples, However, number of samples variate. This can result in a lower performance due to missing data. The same effect is given if subsequent monitoring windows have different durations.
- The module is robust enough to work with missing data by applying and interpolation strategy based on the statistical model being used. This means that tries to correct data assuming they represent normal operation conditions avoiding false alarms in presence of blanks during normal operation conditions, but it could be a cause of miss detections during faulty states.
- The tests have been performed by simulating faults by variations in the load, therefore it is expected that the performance will be better to detect low impedance faults (short-circuits). At the same time, this test validates the feasibility of the module to detect high impedance faults. In that case the existence of previous records will help adjusting some detection thresholds.

4.10. Test and KPI 8: Quality and time needed for awareness and localization of grid faults in LV grid

When a fault occurs in medium voltage (MV) lines it can result in a blackout of not only the MV part of network, but also of all corresponding low voltage (LV) feeders that stem from it and do not have option to operate in islanded mode. In the case of a fault, even approximate localization can be beneficial for repair crews in sense that they do not need to check the entire part of disconnected MV network, but rather the proximity of bus recognized as faulted. With narrowed perimeter of possible fault locations, power restoration can be expedited and network indices such as system average interruption duration index (SAIDI) improved.

In the Figure 30 a single line diagram of the 14-bus MV pilot area is presented, along with the measurement locations of the installed measurement devices. With data collected by PMUs and PQMs it is possible to determine the bus in MV that experienced a fault or is at least the closest one to a fault, should that emerge between two busses.

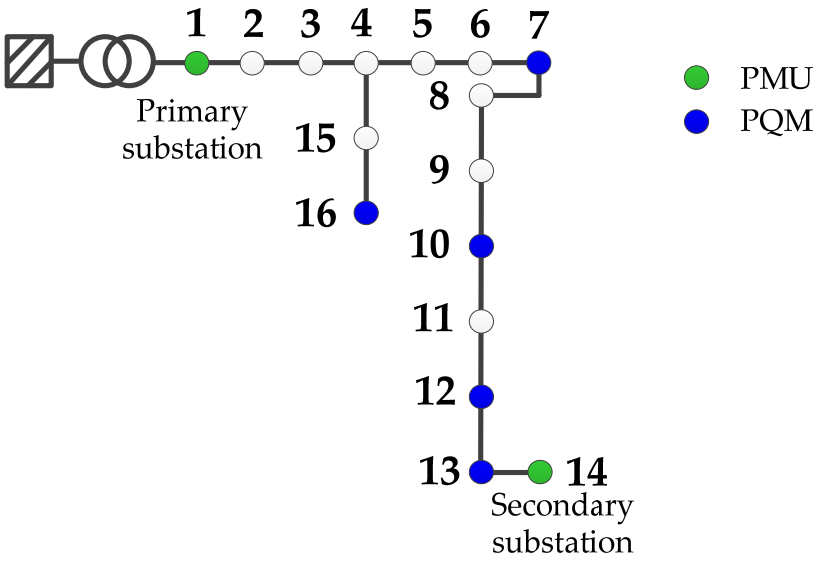

Figure 30 Single line diagram of MV pilot area

The objective of this KPI is to evaluate the quality of fault localization algorithm (FLA) in terms of accuracy, efficiency and elapsed time. Due to no spontaneous fault taking place during the duration of the pilot set-up and the restriction of deliberately imposing a fault in the pilot, the performance of efficiency and accuracy of the algorithm had to be evaluated by means of simulations. The tool that was used for recreating the pilot area in simulation environment was real-time digital simulator (RTDS), which provides the best approximation of the real-life conditions. On the other hand, elapsed time needed by the algorithm was tested in the real-life environment by artificially violating the thresholds of the fault detection.

4.10.1. Followed methodology

As the used FLA returns the bus closest to the fault the error of the algorithm is defined as

$$Error\ [\text{Number of busses}] = |Bus_{calc} - Bus_{act}|,$$

where Bus_{calc} and Bus_{act} are calculated and actual faulted bus respectively. Given that the length of the entire feeder, from primary substation to secondary substation, is ~1.4 km and the distances between adjacent busses range from 12 m to 210 m, we can conclude that each subsequent erroneous bus introduces between 0.86 % and 15 % deficiency in accuracy of algorithm.

Efficiency of the algorithm is defined as

$$Efficiency\ [\%] = \frac{\sum_{i=1}^{N} n_i}{N} \cdot 100,$$

where N is number of all events for which fault location was calculated and n_i is successfulness of algorithm for each particular case (meaning that n_i is 1 or 0 when algorithm was or was not successful respectively).

Lastly, the elapsed time of algorithm is calculated between the fault inception moment and the moment when FLA results are received by DSO. According to Figure 31, this can be expressed as

$$t = t_{stop} - t_{start} = t_1 + t_2 + t_3 + t_4,$$

where t_1 is the time elapsed from the moment that the PMU reports phasors containing the fault, to the moment when fault detection algorithm recognizes the state of a network as faulted. This time includes time for saving PMU measurements to collocated embedded PC and running time of fault detection script, which compares the phasors to predefined thresholds. After the fault is

detected, a trigger is sent from the location of the PMU to the FLA, which is run in the cloud. This time is labelled as t_2. Time t_3 consists of two parts, i.e. the time required to transfer data from the PQMs and the other PMU to the fault localization algorithm and the time of FLA script itself. Finally, the results take some time (t_4) to get from FLA to the network operator centre.

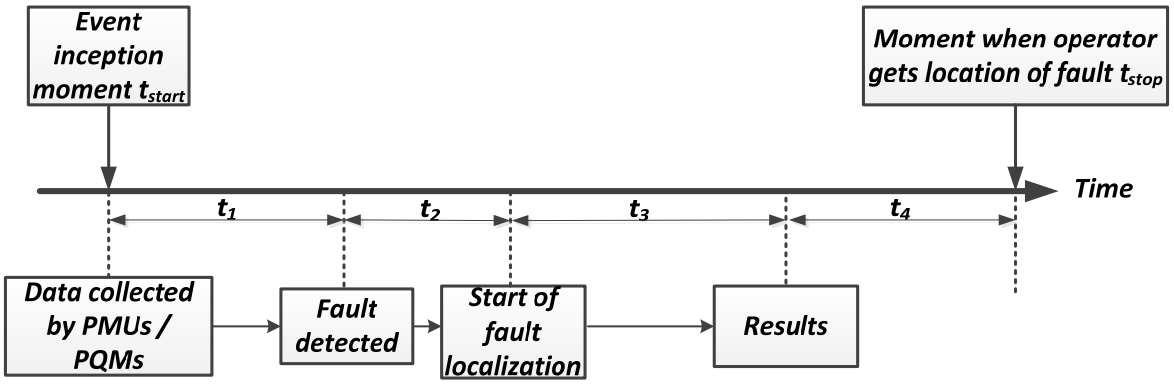

Figure 31 Time delay of FLA components

4.10.2. Calculations and results

In practice the utility's knowledge about system parameters is not precise, also the measurements contain some degree of error. Nevertheless, the robustness of the algorithm can be examined against different influencing parameters as shown in the following tables. For the calculation of accuracy and efficiency of the algorithm in simulation environment the most representative faults were used, i.e. single-phase to ground fault, phase to phase fault and three-phase to ground fault, whereas the Monte Carlo approach was used to generate different scenarios.

- Error in distribution line impedances:

Table 18 shows the results when there are errors in the supposedly known impedances of the distribution lines. For line parameters with up to 5% error the location is always correctly identified. With increased error in impedances, the efficiency of algorithm slightly diminishes, however the results still demonstrate satisfying performance even for error as high as 20%, which is beyond any normal level of error in practice.

Table 18 Performance indications for KPI 8: error in line parameters

Error in line parameters [%]	Correctly identified faulted bus [%]	Immediate neighbor bus identified as faulted [%]	Other bus identified as faulted [%]	Maximum error
5	100	0	0	0 bus
10	97.6	2.4	0	1 bus
15	90	10	0	1 bus
20	78.9	19.7	1.4	2 busses

- Error in Measurements

To discuss the effectiveness of the proposed method against the measurement error of the PMUs two scenarios were examined. The results associated with the error in magnitude measurements and error in angle measurements are show in Table 19 and Table 20, respectively. Note that in order to demonstrate the correlation between the measurement error and fault localization algorithm, the values of PMU measurement errors were exaggerated. In practice the allowed total

vector error (TVE) of the PMU must not surpass the 1% threshold in order for PMU to be compliant with the IEEE C37.118 standard. TVE of 1% equals to 1% error in magnitude measurement or 0.57296° error in angle measurement, meaning that the fault localization algorithm demonstrates satisfying performance with any PMU that is compliant with IEEE C37.118 standard.

Table 19 Performance indicators for KPI 8: error in PMU magnitude measurement

Error in PMU magnitude measurement [%]	Correctly identified faulted bus [%]	Immediate neighbor bus identified as faulted [%]	Other bus identified as faulted [%]	Maximum error
0.1	100	0	0	0 bus
1	99.7	0.3	0	1 bus
2	98.5	1.5	0	1 bus
5	66.7	29.4	3.9	3 busses

Table 20 Performance indicators for KPI 8: error in PMU angle measurement

Error in PMU angle measurement [°]	Correctly identified faulted bus [%]	Immediate neighbor bus identified as faulted [%]	Other bus identified as faulted [%]	Maximum error
0.01	100	0	0	0 bus
0.1	100	0	0	0 bus
1	99.1	0.9	0	1 bus
2	83.5	16.2	0.3	2 busses

Lastly, in order to determine the elapsed time of algorithm, we triggered 100 artificial faults by tweaking the thresholds of fault detection. In Table 21 minimum, maximum and average values for each time component are presented.

Table 21 Minimum, maximum and average time delay values for each component of FLA

Time component	Minimum value [ms]	Maximum value [ms]	Average value [ms]
t_1	1.09	3.46	1.42
t_2	54.92	191.27	71.13
t_3	1384.22	4096.42	1867.86
t_4	57.04	421.74	101.64

With this we can calculate the average elapsed time as:

$$\bar{t} = \bar{t_1} + \bar{t_2} + \bar{t_3} + \bar{t_4}$$

$$\bar{t} = 1.42\ ms + 71.13\ ms + 1867.86\ ms + 101.64\ ms = 2042.05\ ms$$

Conclusion: The average elapsed time from the the fault inception moment and the moment when FLA results are received by DSO is 2.04 seconds. With this the presented FLA method and its execution can be qualified as a near real-time application.

4.11. Test and KPI 9: Quality of LV grid operation in island mode

One of the objectives of this project is to demonstrate the possibility to operate the LV grid in island mode. This type of operation is possible thanks to the energy capacity provided by the batteries in the PED. The island mode could be initiated for self-healing purposes, in case for example of a fault occurred in a point upstream the secondary substation, to reconnect the clients that have undergone the interruption.

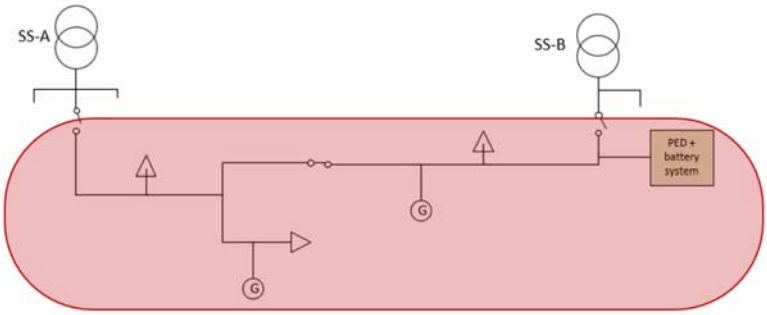

Figure 32 Island mode configuration

Moreover, in the future, the island mode could become a type of normal operation, within the context of energy communities and local markets, for which the independency from the main grid could be initiated for economic/environmental reasons.

4.11.1. Followed methodology

The three sub-indicators will be analyzed as follows:

- Duration: simple measurement of the time elapsing between the beginning and the end of the island.
- Reason for its interruption: analysis and continuous monitoring of the state of the island to identify the cause of its interruption;
- Waveform: analysis and continuous monitoring of waveform quality through the WAMS infrastructure or other power quality analysers installed.

The followed steps for this test were:

- Interruption permission is granted.
- Island mode is initiated following the defined flow and safety standards.
- The pilot area is monitored by the operator through real time data coming from PMUs and PQMs.
- Data about waveform quality is recorded and compared to the standards.
- The island mode ends as planned, the results are recorded.

4.11.2. Calculations and results

As already mentioned, the three main calculations for this key performance indicator are the time (KPI $9_{duration}$), the motive of interruption (KPI $9_{causeinterruption}$) and the waveform (KPI $9_{waveform}$). The obtained results are the following:

$$KPI\ 9_{duration} = \Delta t = 80\ min$$

$$KPI\ 9_{causeinterruption} = [planned]$$

$$KPI\ 9_{waveform} = [fulfilled]$$

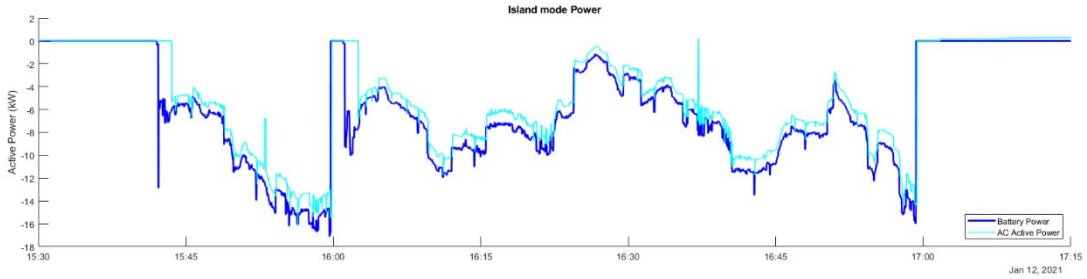

Figure 33 Island power active power, both on AC side and the battery

The island mode was stable for one hour and 20 min without problem starting a planned interruption at 15:40 and finishing at 17:00. It was ended because of power restrictions of the grid. Nevertheless, with the collected data regarding the state of charge of the batteries during this test, it is possible to calculate an approximation of the potential duration time the island mode could be hold.

$$SoC_{start} = 87\%$$

$$SoC_{end} = 54\%$$

$$\Delta SoC_{test} = 33\%$$

$$Potential\ time_{islandmode} = 211\ \text{min} = 3h\ 31\ min$$

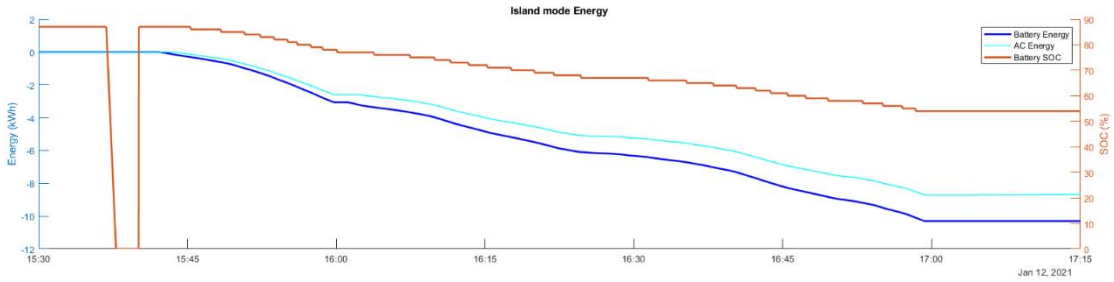

Figure 34 Island mode energy, both on AC side and battery, and state of charge of these

Assuming then steady conditions during the whole period of island mode, and therefore a steady decrease of the state of charge of the batteries, the set up could be operative for 3 hours and 31 minutes, until reaching the whole discharge of the storage system.

4.12. CI 03 Waveform quality in LV grid

This control indicator aims to analyze the waveform quality in the LV grid, in which the RESOLVD technology is installed, to make sure that the standards are fulfilled.

4.12.1. Followed methodology

The control indicator is based on the real measurement of the voltage in order to analyze if it fulfills the current regulation. Note that the measurements should be taken with a power quality analyzer. The power quality analyzer used has been a Chauvin Arnoux CA 8331.

This control indicator considers several aspects which are related to the waveform quality of supplied voltage. Two "sub-indicators" are considered:

1) Fundamental voltage waveform
   - The three-phase values have to be enclosed between 0.9 pu and 1.1 pu at least in 95% of cases according to EN-50160.
   - The three-phase values have to be enclosed between 0.85 pu and 1.1 pu at least in 100% of cases according to EN-50160.
   - The difference among three-phase (using the three-phase indirect sequence values) must be less than 0.02 pu.
2) Non-fundamental voltage waveform
   - The Total Harmonic Distortion of voltage waveforms must be lower than 8% in 100% of cases, according to EN-50160.
   - The Individual Harmonic Distortion of voltage waveforms must be lower than the value indicated in Table 22.
   -

Table 22 Individual Harmonic Distortion limit

Odd harmonics				Even harmonics	
Not Triplen Harmonic		Triplen Harmonics			
Order k	Harmonic voltage (pu)	Order k	Harmonic voltage (pu)	Order k	Harmonic voltage (pu)
5	0.06	3	0.05	2	0.02
7	0.05	9	0.015	4	0.01
11	0.035	15	0.005	6 to 24	0.005
13	0.03	21	0.005	-	-
17	0.02	-	-	-	-
19 to 25	0.015	-	-	-	-

4.12.2. Calculations and results

The data was collected on the 21st of January. The PED was working in island mode from 15:50 until 16:00 (approx.). The grid configuration was 100. It means that PED was feeding only line 2 of SS-B, as can be seen in Figure 35.

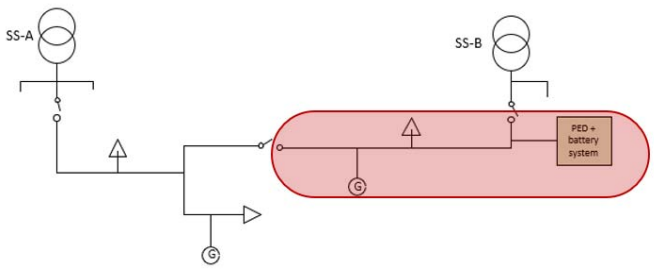

Figure 35 Configuration with SG1 closed, SG2 and SG3 open

Below, in Figure 36, the power (active and reactive), current, and voltage per each phase during the island mode are depicted. These data have been obtained with the PQMs 9 (PED) and 10 (GRID).

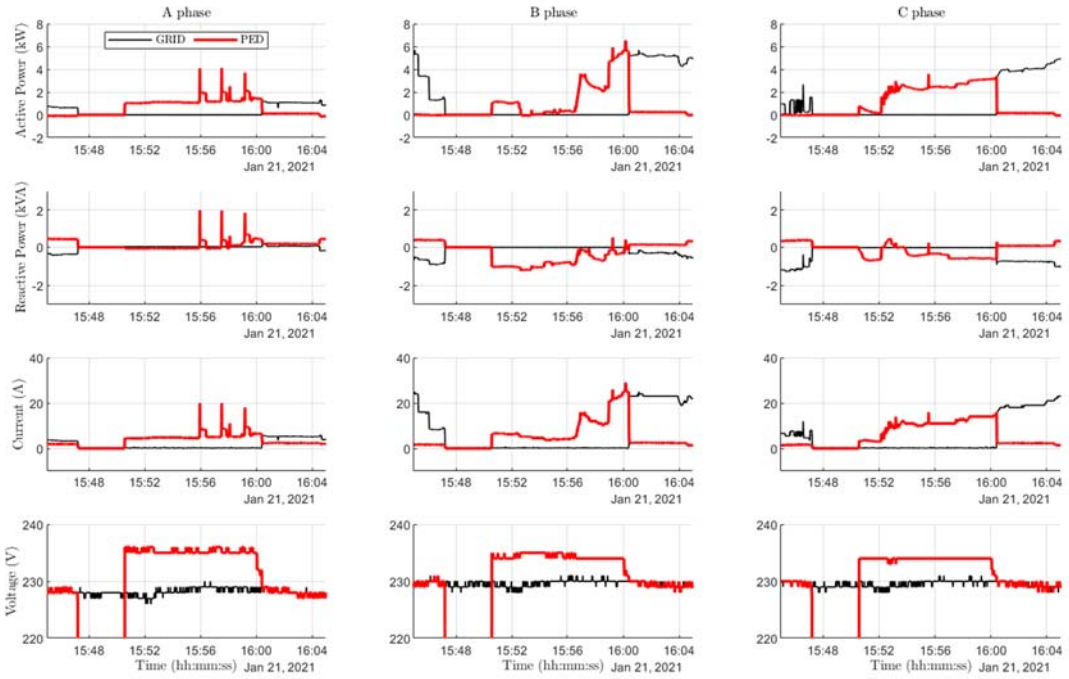

Figure 36: Electrical variable in Island mode

Then, the data obtained with two power quality analyzers (Chauvin Arnoux CA 8331) have been collected. One of the analyzers was installed downstream in order to obtain the voltage quality of the PED working in Island mode. And the other one was installed upstream in order to compare the quality values with the GRID.

In Figure 37, it can be seen how the RMS voltage, the indirect sequence, and the THD remain within limits.

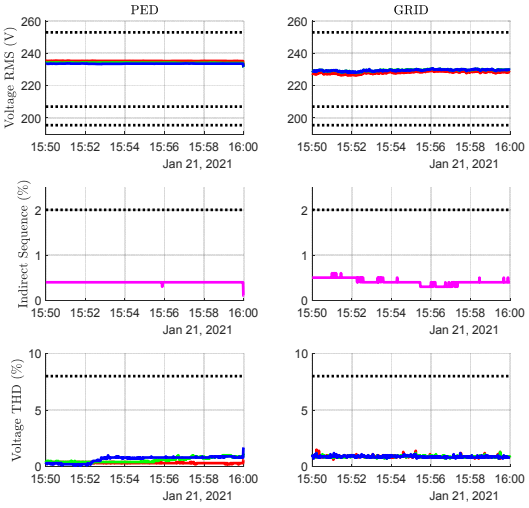

Figure 37: Fundamental voltage metrics.

And in Figure 38 and Figure 39, it can be seen how the odd and even harmonics also remain within limits.

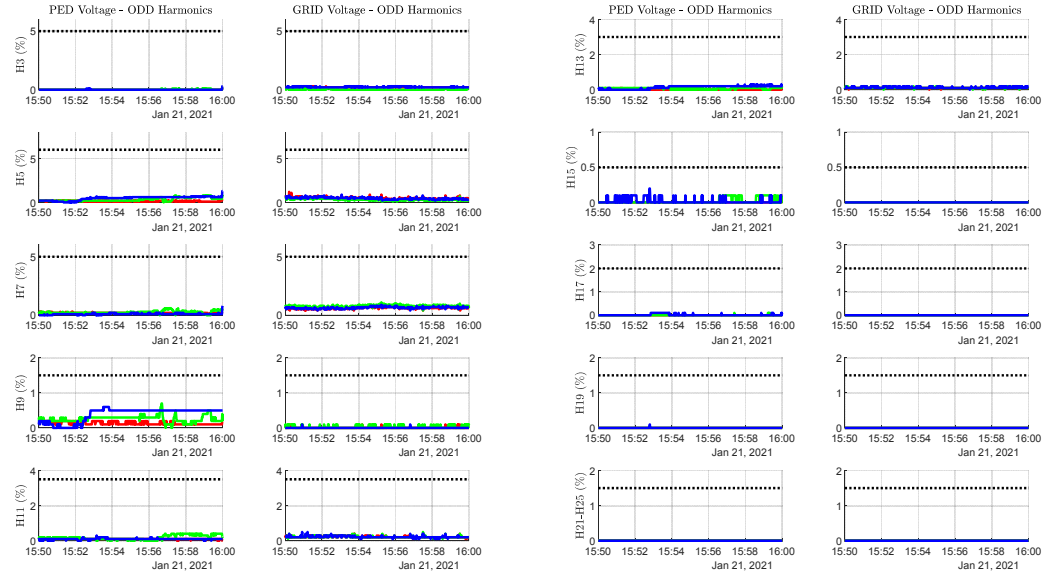

Figure 38: Voltage Odd Harmonics

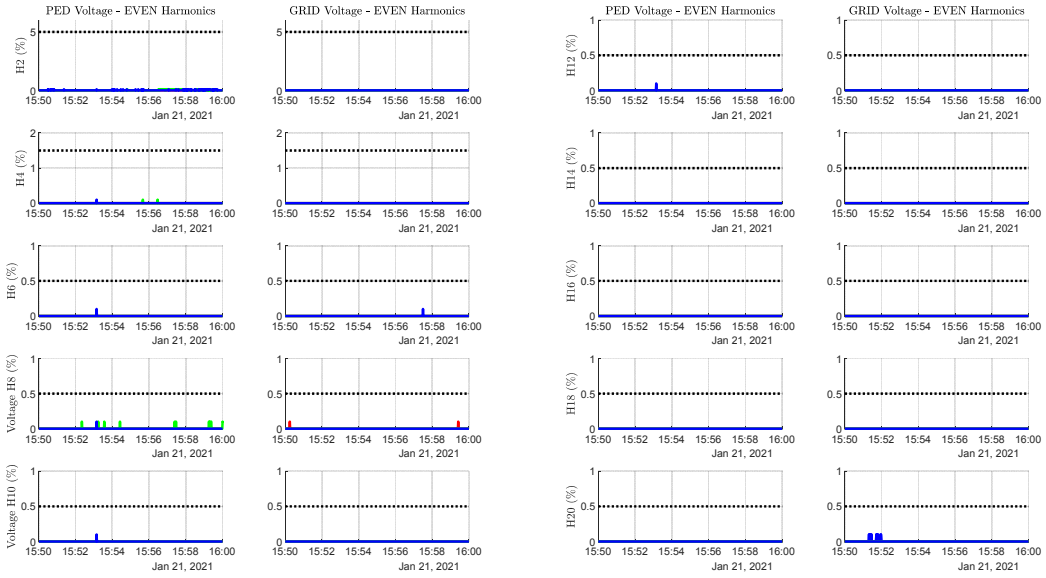

Figure 39: Voltage Even Harmonics

To conclude, it has been demonstrated that the voltage synthesized by the PED accomplishes the waveform quality standards.

This project has received funding from the European Union's Horizon 2020 research and innovation programme under grant agreement No 773715

5. Cybersecurity tests

Cyber security was an integral part of RESOLVD, starting with the security by design approach and the creation of the security guidelines. In this work package, the focus was to validate whether the prescribed measures are in place and correctly configured to ensure security during runtime.

5.1. Methodology

The methodology of the security audit within RESOLVD was based on the level of information and access granted to the penetration tester at JR. This was a two-step process, starting with a black-box text with only minimal information about the system to test. The second step was a gray-box test with some limited information about the system architecture in behind. For that deeper look also credentials and a VPN access has been provided to check the internal setup and security measures of the used components and applications. The structure about the information collected for the security audit can be found in Annex I.

JR utilized a widely adopted approach to perform security assessments that are effective in testing security for services that are provided by the partners. First, the information gathering part focuses on defining the scope of the assessment. Then, services are evaluated and investigated for each system. For this purpose, widely used tools (e.g. nmap, gobuster, Burp, whois, shodan.io, OpenVAS etc.) are used. Once all host services are known, JR conducted tests to detect vulnerabilities in these systems. Therefore, publicly available exploitation databases were queried in order to detect common vulnerabilities. In addition to that, potentially accessible and sensitive files were revealed. Usually, the reason therefore is either a misconfiguration of services or the lack of authentication and authorization mechanisms. Finally, manual tests were carried out by experts in correspondence to the OWASP Top 10 list in search for common vulnerabilities.

The results of these penetration tests were accordingly outlined by JR and for each vulnerable component or application of RESOLVD recommendations to eliminate the identified security issues as well as individual advices were communicated to the responsible partners. This was done by creating individual confidential documents for each partner system with the following document structure:

.

- Summary
- Recommendations
- Methodology
- Information Gathering & Scope
- Penetration
- Service Enumeration
- Exploitation
- Whois/Shodan Result
- House Cleaning
- Appendix
- Individual reports produced by used pentest tools

5.2. Results

During the assessment, several vulnerabilities and attack vectors were identified for the different components and for each of them corresponding fixes or mitigation strategies were provided. The following list gives an overview of the weak points found without claiming to be a complete list of found vulnerabilities.

Table 23 Excerpt from the list of found vulnerabilities

Vulnerability	Background	Mitigation Strategy
Weak TLS cipher suites were used	Even if a TLS certificate is used there are weak cipher suites for the older versions of TLS1.1 and TLS1.2 which are considered to be broken and therefore not secure anymore.	Usage of TLS 1.3 or usage TLS 1.2 with one of the following cipher suites by enabling also authentication and integrity. • DHE_RSA_WITH_AES_128_GCM_SHA256; • ECDHE_RSA_WITH_AES_128_GCM_SHA256; • DHE_RSA_WITH_AES_256_GCM_SHA384; • ECDHE_RSA_WITH_AES_256_GCM_SHA384
Information disclosure due to default pages	These pages give the attacker an idea which system is used in the background	Do not reveal any (default) configuration and pages to the users. Instead, give a valid index page or a 404-error page.
Out of date third party libraries	Outdated third party libraries which are not patched might have multiple (known) vulnerabilities	The used versions … are prone to multiple vulnerabilities. An upgrade to the latest versions is therefore recommended.
Missing password policy	Weak passwords can be guessed, and brute forced by attackers. This is one of the easiest and most common attack vectors on how attackers get initial access to a system	Implement and validate a strong password policy. To do so, follow the latest version of the recommendations of the NIST or the OWASP guidelines.
Authentication bypass	Access to the system without authentication possible	Fix SQL injection by using parametrized queries and input validation
Upload of any data by unauthenticated users	An upload of any data via an API service could trigger several different attacks.	Make sure to validate uploaded data from any user. Also make sure to validate the authenticateToken parameter correctly
Cross Site Scripting (XSS)	If there is some input field which is not secured an attacker can reflect the user input and therefore able to execute Java Script code for the user	Use input validation and output encoding to validate any input (regardless of user input or input from another service) that is made to the … file.
Reveal of session tokens	If in a stateless protocol, session identifiers are used to identify a session and a series of related message exchanges this information can be revealed.	API should not reveal session tokens as GET parameters. Instead, use the POST method when submitting session tokens.
Disclosure of information due to development remainders	Files containing development remainders such as comments, debugging info, debugging URLs, etc. can disclose important information to the attacker.	Make sure to delete any development remainder at the live system to avoid information disclosure

The Results of the security check exposed the importance of such audits, even if RESOLVD applied the security be design approach and performed some interactions during development. It

turned out that the specified security guidelines were only partially implemented or were also overturned by incorrect configuration settings on the deployed system. Therefore, an essential recommendation for future derived from this is that the interaction and communication between software developer, testers and cyber security experts should be performed more often to mutually increase the awareness of both sides.

6. Future opportunities

After presenting all the performed tests and the obtained results, it is worth it to dedicate a section to mention the limitations that have been encountered along the testing phase, that leave room for improvement and further experimentation with the developed technology.

The first condition that was encountered when testing, was the limitation of storage capacity, due to the malfunctioning of part of the batteries, in specific the Lead Acid. This has limited the testing potential to the capacity of the Lithium-ion batteries (30 kWh), when it could have been of 48 kWh. With this in mind, it can be said that the KPI 9 regarding the test of island mode of the LV grid, can provide higher results if tested in the future with the full batteries capacity. Moreover, other calculated KPIs that have taken into consideration energy consumption of the PED and the batteries, would also need to be recalculated with the Li-ion batteries operative, since this value would then slightly increase.

Another factor to take into consideration for further improvement, is the issues encountered regarding the communication between the ILEM and the PED. This link was not found to be stable for a long enough period to be able to test some scenarios for more than some hours or few days when the initial plan was to set up tests for a week period. This is planned to be further investigated and fixed in the following months, since this technology will be further used in another European project, FEVER.

Finally, the main hardware asset that has been developed with the RESOLVD project, the PED, has further potential to be matured before its readiness for market. After the project, this technology can increase its performance and value by adding new services and capabilities or upgrading its robustness. Overall, the goal is to achieve a higher technology readiness level (TRL) to be able to industrialize the technology, reduce its price and turn what is now a first prototype into a fully competitive and profitable device, following the timeline shown in Figure 40Figure 40.

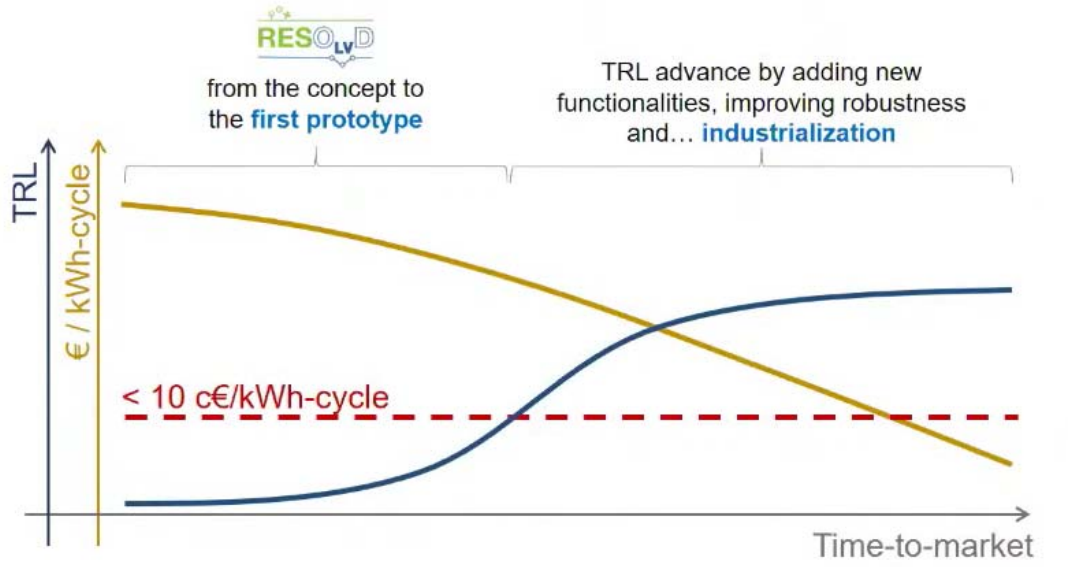

Figure 40 Time-to-market timeline of the PED technology

7. Conclusions

After the testing period and resulting calculations of the different key performance indicators, several points can be positively concluded.

From the loss's reduction point of view, it can be safely said that the actuation of the PED has decreased the amount of power used per unit of resistance in the line, by improving the waveform quality, compensating reactive currents, harmonics or balancing the 3 phase currents. It has also been possible to reduce power losses by shifting peaks in low voltage lines, achieving a reduction on 18% of these high points and a 43% reduction of the variability of the curve. A generalized reduction of peaks at the low voltage grid provides a substantial increase in efficiency of the power system, since the transport losses depends on the square of the current, and therefore a consequent reduction of emissions, according to the energy mix. On the other side, it has been calculated that the PED together with the batteries represent around 6% of the total energy managed, which leads to an increase of the total energy of around 4%. This is due to the oversized design the PED has, to be able to manage larger power peaks, and because of that increase of consumption, is recommended to limit the GOS operation only when the excess of PV generation is enough to compensate these extra energy use.

Regarding the economical competitivity of the developed technology, it has been seen that when compared to a standard or traditional infrastructure investment, it is still more expensive to install the RESOLVD technology. This is because the technology is still in a prototype level and is believed that its cost will decline once it achieves a ready-to-market and industrialized phase.

When it comes to over/undervoltage issues and how the technology deals with them, the tests proved that the injection and consumption of active and reactive power have a direct effect on the voltage level of the lines, increasing when the PED is set in generation mode, and decreasing when it is set to load mode. Thus, schedule of charge/discharge of batteries can be used to control voltage variations and reverse power flow during the day when large differences between demand and generation occur.

Moreover, the technology has also been tested to predict critical events in the grid like congestions. Nevertheless, due to variations on the pilot regarding the loads, the event forecasting capability was evaluated by downsizing the ampacity of a line segment and changing the configuration of the grid to get the maximum current flowing through this segment, and therefore the performance of this service was measured in terms of effectiveness and considering only artificially created congestions. The CEPA did indeed identify critical events during the test and the GOS successfully provided a solution with the minimum switching operations.

As with critical events, the detection of faults such as deviation of voltage or currents nominal values was also tested by generating artificial scenarios to be identified as these abnormalities. It can be concluded that the accuracy of this detection application is around 97%, even though a delay between the detection and the informing points can be notable.

Finally, after having the pilot area working under island mode for more than one hour, it is safe to say that the RESOLVD technology successfully operated as voltage sources, feeding consumers directly from the storage system.

Taking into consideration the technical limitations for all the tests and calculations, and to summarize and gather all the results obtained from these tests, Table 24 provides the generic picture of the main outcomes.

Table 24 Summary of KPI and results obtained

KPI-01	Power loss reduction due to waveform quality improvement	166,7 W/Ω
KPI-02	Improvement of the energy profile in the secondary substations	Avg peak reduction: 18% Avg curve variability reduction: 43%
CI-01	Efficiency rate of the PED and the energy storage system	Global charging efficiency: 95.4% Global discharging efficiency: 93.4%
KPI-03	Increase of DERs hosting capacity in LV network	36,95%
KPI-04	Reduction of DSO investment.	-61,55% -15.985,3 €
CI-02	DSO operation expenditures with respect to the BAU solutions	2.280 €/year
KPI-05	Percentage of improvement in line voltage profiles with power injection and consumption	3%
KPI-06	Rate of prevented critical events in the LV grid due to forecasting and remote control of grid actuators	The results from the tests carried out have permitted to adjust voltage variations among secondary substations
KPI-07	Quality of online event detection in LV grid	-Accuracy: 97,1% -Precision: 92,6% - Miss Detections: 0% -False Alarm Rate: 4,39%
KPI-08	Quality and time needed for awareness and localization of grid fault MV grid	Time between fault inception and reception of FLA results by DSO: 2.04 s
KPI-09	Quality of LV grid operation in island mode	- Duration: 80 min - Reason for island mode interruption: planned - Waveform quality: fulfilled
CI-03	Waveform quality in LV grid	Quality standards fulfilled

Alongside with the operational test, the cybersecurity evaluation provided the partners with recommendations to eliminate security issues as well as individual advices.

All in all, it can be said that robustness of the technology has been achieved by a full electrical integration on the secondary substation of the DSO, with a main hardware component, the PED, performing with an efficiency of 94.4%. Moreover, there is fully interoperability, enabled by a setup of applications and communication channels to remotely operate from DSO's SCADA. The developed technology, both hardware and software, have provided promising results to keep

further working on the next generation of innovative technologies to enable smart grids, storage and energy system integration with increasing share of renewables.

This project has received funding from the European Union's Horizon 2020 research and innovation programme under grant agreement No 773715

Annex I: Security Audit Questionnaire

In order to perform the security audit, please fill out the following form to the best of your knowledge. If any help or additional information is needed, please contact JR.

The methodology of the security audit will be a black box and in further steps, a grey box test. This is done in order to cover most of the possible attack scenarios – therefore credentials, and a VPN access if needed, shall also be provided.

A report of the found security vulnerabilities including all steps performed, as well as a mitigation strategy to address the vulnerabilities will be sent out once the security audit was performed.

DISCLAIMER

As this questionnaire contains sensitive information, it is important that this document is treated confidentially.

Access to Services

Please specify VPN information in the following table, if needed for accessing your services.

VPN Address	Port	Credentials
Additional Comments:		

Please insert any RESOLVD system that is operated by your institute. Please also specify in the additional comments any notes that might be useful.

URL	IP Address	Service	Port (TCP/UDP)	Connection Type (LAN, WLAN, etc.)	Credentials	VPN
Additional Comments:						

If any external data resources are used for your systems, please specify them in the following table. This is needed to address possible attacks, that could be hidden in certain data formats when the service has no proper input validation.

External Service	Internal Service	Usage	Data Format
Additional Comments:			

Permission Memo

A permission memo is an agreement that defines the scope (IP addresses, services, hostnames), the date and time when the audit is performed, and other legal matters (such as partners will not disclose any information, etc.). This agreement is signed by involved partners in beforehand. Please tick the boxes below if we should send you a permission memo in beforehand.

☐Yes, we need a permission memo

☐No, we do not need a permission memo

Date

JR scheduled the second week of November until the second week of December for the security audits (dd.mm.yyyy – dd.mm.yyyy). If you and your IT department need to know a specific date in beforehand, we can arrange this. Please tick the boxes below if we should schedule a specific date for you – we can agree this then via mail bilateral.

☐Yes, we need to arrange a specific time.

☐No, we do not need a specific date – the range from dd.mm.yyyy – dd.mm.yyyy is fine.